SPECIES DISTRIBUTION MODELS FOR THREE DEEP-SEA CORAL AND

SPONGE TAXA IN THE SOUTHERN CALIFORNIA BIGHT

By

Nissa Kreidler

A Thesis Presented to

The Faculty of Humboldt State University

In Partial Fulfillment of the Requirements for the Degree

Master of Science in Natural Resources: Fisheries

Committee Membership

Dr. Andre Buchheister, Committee Chair

Dr. Mark Henderson, Committee Member

Dr. Tim Bean, Committee Member

Dr. Brian Tissot, Committee Member

Dr. Erin Kelly, Graduate Coordinator

December 2020

ABSTRACT

SPECIES DISTRIBUTION MODELS FOR THREE DEEP-SEA CORAL AND
SPONGE TAXA IN THE SOUTHERN CALIFORNIA BIGHT

Nissa Kreidler

Deep-Sea Coral and Sponge (DSCS) species are signature taxa of deep-water habitats,

however understanding the ecological mechanisms that drive their geographic

distributions can be difficult to uncover due to the challenges of surveying deep-water

ecosystems. A recent study on benthic assemblages in Southern California revealed

statistical associations between several DSCS and demersal fishes, many of which are

important to management agencies due to commercial or conservation concerns. Maps

that predict where these DSCS may occur are needed for the management and protection

of these DSCS taxa and the fauna that rely on them for habitat. In this thesis, I develop

predictive models and maps for three DSCS in the Southern California Bight, *Antipathes

dendochristos, Plumarella longispina,* and an unidentified Porifera sponge. Two of the

taxa, *P. longispina* and Porifera have been identified to be associated with young-of-the-

year rockfish in a previous study. Predictive maps were created using species distribution

models developed with habitat-related variables (e.g. food availability, depth, and

bathymetry). Generalized Additive Models (GAMs) were created using the best practices

for developing DSCS species distribution models, which includes accounting for spatial

auto-correlation and model uncertainty. I provide a comparison of how these model

results differ from the results of a commonly used modeling approach, Maxent, that relies

on presence-only data. Both GAMs and Maxent models performed well when predicting known occurrences, but the variables deemed most important in those models differed. Predictions using GAMs found that all three taxa were distributed in patches across the study region and that the covariates that predicted species distributions were similar between the three taxa. Specifically, species distributions primarily relied on depth, northern currents, and eastern currents. Maxent predictions were much more constrained throughout the study area, with high suitability found mostly on the fringes of the islands off the coast, and covariates relationships were more variable between species. When the GAMs were constrained to the areas where the model had low uncertainty (Bayesian credible interval ranges < 0.25), the predicted species distributions were more similar between the two modeling methods. High probability of DSCS occurrence exist both inside and outside the Channel Islands National Marine Sanctuary (CINMS), with large areas occurring beyond sanctuary boundaries, mostly north of Santa Barbara Island, around Santa Catalina and San Clemente Islands, and along the coast near San Diego. These areas may be important for future explorations and conservation considerations.

ACKNOWLEDGEMENTS

Research and Exploration, especially Andy Lauermann for sharing your knowledge of deep-sea coral with me, and to Heidi and Greta for forever listening to me talk about my thesis. Thank you to Chris Caldow and Lizzie Duncan at the Channel Islands National Marine Sanctuary for discussing the project with me and "deepening" my appreciation for deep-sea corals.

Lastly, thank you to my family and friends. My Kreidler-States family has provided unending support and love and I could not have done this work without you. Most of all, thank you to Jack for always being there and bringing home the chicken wine, and to our fur child, Sir Toddrick, who was a daily reminder that life is better at the beach.

TABLE OF CONTENTS

LIST OF TABLES

LIST OF FIGURES

LIST OF APPENDICES

INTRODUCTION

Deep-Sea Coral and Sponge Species (DSCS) are some of the longest-lived marine species and their complex, three-dimensional structure provides habitat for demersal fish and other invertebrates (Fossa et al., 2002; Baillon et al., 2012; Stone, 2014). Due to their slow-growing and sessile nature, DSCS are highly susceptible to destructive fishing practices and climate change (Freiwald and Roberts, 2005; Dodds et al., 2007; Gugliotti et al., 2019). DSCS known occurrences, estimated distributions of their ranges, and biological requirements have become important to marine management and a focus for current research (Hourigan et al., 2017; Caldow et al., 2019; Winship et al., 2020). Studying DSCS is difficult due to the high cost of deep-sea surveying and their sensitivity to translocation (Boch et al., 2019), thus some of the biological needs and mechanisms of these organisms has been inferred from statistical models in addition to estimates of their distributions (Huff et al., 2013; Ross and Howell, 2013). In this study, I develop predictive models and maps for DSCS distributions off the coast of southern California and explore the relationships between these distributions and the environmental and habitat conditions that predict them. Special reference is made to the amount of habitat that occurs inside the Channel Islands National Marine Sanctuary (CINMS), and a comparison between the results of two different modeling methods.

Deep- Sea Coral and Sponge Ecology

Habitat requirements dictate where DSCS are found and are connected to biological processes. DSCS often occur in areas with enhanced currents that flush accreted sediment and deliver a reliable food supply (Freiwald and Roberts, 2005; White et al., 2005). As filter feeders, DSCS rely on organic matter and near surface phytoplankton and zooplankton that are delivered via currents to benthic habitats (Henrich et al., 1997; Mortensen, 2001; Duineveld et al., 2004; Kiriakoulakis et al., 2005; Davies et al., 2009). DSCS also require hard substrate to attach to and are found in waters between 4° and 12°C (Freiwald and Roberts, 2005).

DSCS act as habitat themselves, providing nursery grounds for rockfish and other demersal fishes (Fossa et al., 2002; Baillon et al., 2012; Stone, 2014). They have been shown to serve as habitat for eggs and juveniles of several fish species including commercially important rockfish species (*Sebastes spp.*) in Canada (Baillon et al., 2012), the Aleutian Islands of Alaska (Stone, 2014), the coast of Norway (Fossa et al., 2002), and California (Henderson et al., 2020). In Hawaii, the black coral *Antipathes dichotoma* was found to provide habitat for 40 fish taxa (Boland and Parrish, 2005). Rockfish in Cordell Bank, California were also found to be more frequently present with DSCS than not (Pirtle, 2005), which is similar to the association between DSCS and fish assemblages in the Southern California Bight (SCB) (Henderson et al., 2020).

Dense patches of DSCS can be hot-spots of biodiversity and provide important structures for fish habitat (Lumsden et al., 2007; Lessard-Pilon et al., 2010), and recent

research points to strong associations between fishes and DSCS in the SCB (Henderson et al., 2020). While empirical associations between fishes and DSCS populations are not always clear (Auster, 2005; Tissot et al., 2006), Henderson et al. (2020) show that some rockfish species, including the recovering Bocaccio rockfish (*Sebastes paucispinis*), are significantly associated with DSCS in the SCB. These findings are important for elucidating relationships between fishes and DSCS, which are both at risk due to anthropogenic disturbances. Henderson et al. (2020) identified 13 taxa of DSCS that increased the likelihood of 14 species of adult and young-of-the-year rockfish (*Sebastes* spp.) presence (Table 1). These results were based on logistic regressions that modeled the presence of fish species relative to biotic (e.g. DSCS presence and size) and abiotic (e.g. substratum and temperature) variables. For example, a one standard deviation increase in the presence of the flat sponge (Porifera #2), increased the presence of pygmy rockfish (*Sebastes wilsoni*) by 35% (Table 1) (Henderson et al., 2020).

Table 1. Thirteen DSCS and associated *Sebastes* taxa with percent increase in the probability of fish presence with one standard deviation increase in DSCS density based on the logistic regression models of Henderson et al. (2020). *Sebastes* taxa of management and conservation concern are identified in bold.

DSCS Type	DSCS Species	Associated Fish Species	% increase
Coral	*Acanthogorgia spp.*	***Sebastes rufus***	15%
	Adelogorgia phyllosclera	*Sebastes miniatus*	12%
		Sebastes wilsoni	11%
		Sebastes umbrosus	10%
	Eugorgia rubens	*Sebastes chlorstictus*	11%
	Farrea occa	*Sebastes simulator*	14%
	Plumarella longispina	***Sebastes spp. YOY***	7%
		Sebastes rufus	9%
	Plumerella longispina	***Sebastes spp. YOY***	9%
Sponge	*Haliclona (gellius)*	***Sebastes rufus***	12%
		Sebastes ensifer	12%
		Sebastes wilsoni	10%
	Plexauridae #1	*Sebastes semicinctus*	31%
	Porifera sp. #1	*Sebastes miniatus*	20%
		Sebastes ovalis	23%
		Sebastes wilsoni	29%
	Porifera sp. #2	***Sebastes spp. YOY***	15%
		Sebastes levis	16%
		Sebastes simulator	11%
		Sebastes constellatus	20%
		Sebastes hopkinsi	28%
		Sebastes wilsoni	35%
	Porifera sp. #3	***Sebastes spp. YOY***	9%
		Sebastes rufus	12%
		Sebastes levis	13%
		Sebastes miniatus	22%
		Sebastes rubrivinctus	14%
	Porifera sp. #5	*Sebastes jordani*	26%
	Rhabdocalyptus dawsoni	***Sebastes rufus***	24%
		Sebastes ensifer	7%

Protecting DSCS and their habitat may be critical to sustain the overall health of the SCB ecosystem, but DSCS are highly sensitive to destructive fishing practices such as bottom trawling (Freiwald and Roberts, 2005; Heifetz et al., 2009; Pham et al., 2014; Yoklavich et al., 2018). In Alaska, surveys found that 14% of corals and 21% of sponges were damaged and that disturbance to the seafloor from fishing gear was widespread (Heifetz et al., 2009). Likewise, 45% of bamboo corals showed signs of trawling damage along the northern California border (Yoklavich et al., 2018). The SCB is a similarly disturbed ecosystem characterized by heavy coastal development, runoff, and a history of overfishing (Love et al., 1998, 2009). DSCS that are present off the coast of southern California may be important to the recovery and persistence of fish and other deep-sea fauna, given the role of DSCS as benthic fish habitat (Etnoyer and Warrenchuk, 2007).

Many commercial fisheries rely on the SCB as it is the boundary for many northern and southern fish ranges (Moser et al., 2000); however, overexploitation of the SCB has led to the collapse of multiple fisheries (Dayton et al., 1998; Erisman et al., 2011). Efforts have been put forward to conserve these fisheries, including marine protected areas and a widespread ban on bottom trawling. For example, the Channel Island National Marine Sanctuary (CINMS) was created in 1980, and is managed by the National Oceanic and Atmospheric Association's (NOAA) Office of National Marine Sanctuaries (ONMS, 2009). In 2018, an amendment to Pacific Coast Groundfish Fishery Management Plan closed the majority of the SCB to bottom-contact fishing, such as bottom trawling (NMFS, 2019).

Advantages of Mapping and Modeling

Monitoring of deep-sea communities is important for conservation of biodiversity and essential fish habitat, but surveys are expensive and challenging. Due to difficulty in monitoring these habitats, standard sampling methods such as trawls, submersible and ROV dives have been used to obtain more detailed information on fish and DSCS abundance and distribution (Love and Yoklavich, 2008; Love et al., 2009). Extensive submersible dive trips over the last two decades have provided a wealth of information on the relationships between DSCS and their associated fauna (Yoklavich and Love, 2005; Love and Yoklavich, 2008; Love et al., 2009; Huff et al., 2013), but it is infeasible to survey the entire seafloor of the SCB. Surveying DSCS communities is a complicated, highly technical, and costly process (Yoklavich and O'Connell, 2008). Submersible operations can cost upwards of $11,000 per day (Yoklavich and O'Connell, 2008), which is generally prohibitive for conducting extensive surveys on deep-sea communities.

Mapping the potential for DSCS habitat and their associated species can be a cost-effective way to leverage existing data and provide information to natural resource managers without excessive field survey costs. The Magnuson-Stevens Fishery Conservation and Management Reauthorization Act of 2006 addressed the growing body of knowledge on DSCS as potential Essential Fish Habitat (EFH) by creating a program specific to DSCS (Lumsden et al., 2007), which explicitly identifies locating and mapping DSCS communities as a top priority. Predicting where corals may occur based on environmental parameters has been conducted regionally for the west coast of North

America (Bryan and Metaxas, 2007; Guinotte and Davies, 2014), east coast (Bryan and Metaxas, 2007) and globally (Tittensor et al., 2009; Davies and Guinotte, 2011; Yesson et al., 2012), but a local predictive model for multiple DSCS and sponge species does not yet exist for the SCB (Huff et al., 2013).

<div align="center">Species Distribution Modeling</div>

Species Distribution Models (SDMs) are used to predict species occurrences across a landscape based on known occurrences and the environmental conditions at those locations. These models can then be used to predict occurrences in new areas, or make predictions of how species distributions may change based on projected changes in habitat conditions. Some models use presence and absence data using standard field surveys, whereas other models can be developed using presence-only data when absence data is lacking. SDMs have been used extensively in conservation management, including where to focus conservation efforts (Kariyawasam et al., 2017; Bazzichetto et al., 2018), making predictions for species distributions under future climate conditions (Nakao et al., 2013; Ohashi et al., 2016), and directing future research efforts (Huff et al., 2013; Caldow et al., 2019). SDMs for predicting DSCS have become prevalent in the last ten years and will be critical in conservation and understanding DSCS moving forward (Hourigan et al., 2017; Winship et al., 2020). In this study I use SDMs to make predictions of where DSCS are likely to occur in the SCB, and compare two different SDM methods.

Research objectives and value

In this thesis, I used species distribution models to make predictive maps for three DSCS in the Southern California Bight: the black coral *Antipathes dendochristos,* gorgonian *Plumarella longispina,* and an unidentified sponge species (also identified as Porifera #2 or "flat sponge" by the Southwest Fisheries Science Center. These taxa were selected for two main reasons: (1) *P. longispina* and Porifera sp. are significantly associated with young-of-year (YOY) rockfishes in Henderson et al., (2020) and (2) *A. dendrochristos* was modeled by (Huff et al. 2013). This previous model for *A. dendrochristos* used the same dataset the data in this study, which will allow for further comparison between our methods. Creating predictive maps for the taxa associated with YOY rockfish will provide important information on areas that are connected to the health and abundance of fisheries and the greater ecosystem. YOY are particularly important in defining Essential Fish Habitat and that is worth mentioning.

Accordingly, the specific objectives of this study were to: (1) create species distribution maps of suitable habitat for these three taxa, (2) identify environmental variables that best predict their distribution, (3) compare differences in predicted distributions based on two modeling approaches, and (4) compare the amount of high suitability area inside and outside of the CINMS. CINMS has expressed a need to know where these DSCS species occur and providing predictions to them may help facilitate future research efforts (CINMS, 2012; Caldow et al., 2019). These models are the first SDMs to include DSCS food availability at depth, which was expected to be an important

factor for DSCS. Predictive maps help provide missing information on DSCS habitat

suitability in the SCB. This work extends current knowledge of DSCS that are known to

be associated with commercially important demersal fishes. These maps also provide

baseline data on sensitive deep-sea habitat and reveal highly suitable areas that could be

prioritized for future surveys and protection.

MATERIALS AND METHODS

Study Site

The Southern California Bight is an open embayment that extends from Point Conception to San Diego (approximately 121° W, 34.5° N to 117° W, 32° N) (Figure 1) and contains diverse habitats to over 500 species of fishes and 5000 benthic invertebrate species (Dailey et al., 1994). Several islands, basins, and ridges exist in the SCB that affect circulation patterns at all depths (Hickey et al., 2003). The southeastward California Current and Southern California Countercurrent create a cyclonic circulation pattern within the SCB that may enrich and retain the faunal communities in the SCB in addition to increasing upwelling created around the Channel Islands (Lynn and Simpson, 1987). Generally strong upwelling occurs in winter and early spring, with some advection of nutrients and productivity from outside the SCB in summer and fall (Hickey, 1992).
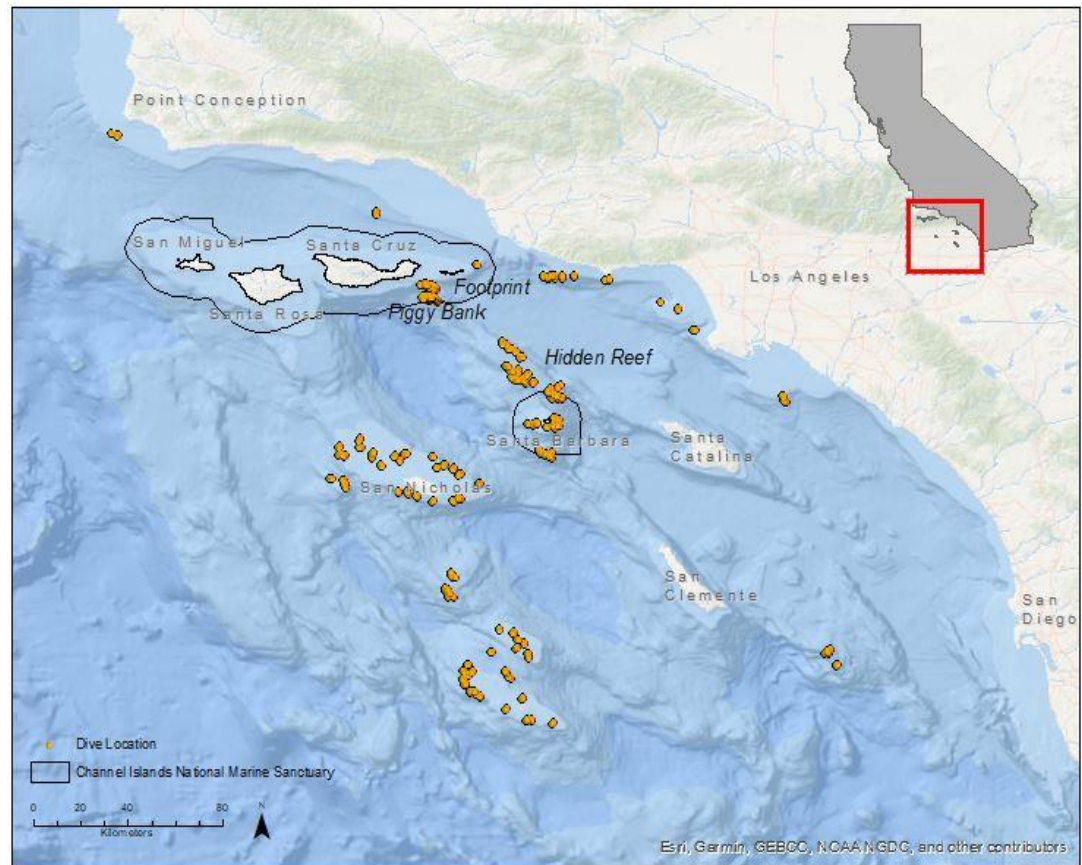
Figure 1. Study site in the Southern California Bight, bound by Pt Conception in the north and San Diego in the south. Dive sites are denoted by orange dots, National Marine Sanctuary boundaries outlined in black. Dive sites= 164.

Multiple marine protected areas exist in SCB, including those managed by the state (CDFW) and federal (NOAA) governments. The CINMS is a federally protected area that encompasses San Miguel, Santa Rosa, Santa Cruz, and Anacapa Islands in the north and Santa Barbara Island in the south. CINMS covers about 3971 square kilometers, of which 2679 square kilometers (~67%) occurs between 50 – 500 m.

Data Acquisition

This study used 11 years of video data collected using two occupied submersible, *Delta* and *Dual Deepworker,* from 1999 to 2010 in the SCB. A total of 164 dives were completed, both inside and outside of the CINMS (Figure 1). The average depth of dives was 194 m, with the minimum dive depth occurring at 24 m, and maximum depth at 867 m. Data used for model construction was limited to dives between 50 m to 500 m to be consistent with the methods used in Henderson et al. (2020). The average depth of these restricted dives was 223 m. Two-meter-wide submersible transects were conducted 1 m off the seafloor at speeds roughly between 0.5 and 1 kt. Video footage was collected using a camera mounted outside the submersible, which was later analyzed by the Habitat Ecology Team at the Southwest Fisheries Science Center for species identification, count, and size. Data was stored and managed by the Habitat Ecology Team and has been utilized by multiple studies to address different research questions with different analytical methods (Tissot et al., 2006; Love and Yoklavich, 2008; Love et al., 2009; Huff et al., 2013; Henderson et al., 2020).

Environmental Variables

A total of nine environmental variables were explored for the SDMs because they have been hypothesized or documented to influence the distribution of DSCS taxa of interest. These variables include (1) northward and eastward bottom currents, (2) temperature, (3) dissolved oxygen, (4) diatom concentration, (5) detritus concentration,

(6) depth, (7) slope, (8) broad scale Bathymetric Position Index (BBPI), and (9) fine scale

Bathymetric Position Index (FBPI) (Table 2).

Table 2. Environmental variables used in quantitative models. Asterisk denotes final non-collinear variables used in model fitting.

Variable	Unit	Definition	Source
Depth*	Meters	Seafloor bathymetry based on multibeam sonar surveys	California Relief Model
BBPI*	-	Broad Bathymetric Position Index at 20 km. Difference between individual cell depth and the average depth of surrounding neighborhood.	California Relief Model
FBPI*	-	Fine-scale Bathymetric Position Index at 250 m	California Relief Model
Slope*	Degrees	Average difference between cell depth and nearest three neighbor cells (90 m)	California Relief Model
Diatom*	mmol N per m^3	Average concentration of diatoms available at depth	ROMS/NEMURO
Detritus	mmol N per m^3	Average concentration of detritus available at depth	ROMS/NEMURO
Temperature	°C	Average bottom temperature	ROMS/NEMURO
Dissolved oxygen	mmol N per m^3	Average dissolved oxygen	ROMS/NEMURO
Bottom currents*	Velocity (m/s)	Average northward and eastward current velocities	ROMS/NEMURO

Environmental variables are difficult to obtain for the deep ocean, so this study utilized

output from a biogeophysical model to estimate the environmental conditions at depth:

the Regional Oceanographic Modeling System coupled with the North Pacific Ecosystem

Model for Understanding Regional Oceanography (ROMS/NEMURO). The

ROMS/NEMURO model provided three dimensional estimates of biogeophysical

elements including current velocity, carbon and nitrogen concentration, and

phytoplankton and zooplankton abundance (Moore et al., 2011; Edwards et al., 2015;

Song et al., 2016). The California ROMS/NEMURO model estimates ocean conditions

from 30° to 48° N, and from the coast to 134° W (Broquet et al., 2009; Veneziani et al.,

2009). Satellite sensors and *in situ* sources of assimilated data constrain the model, which

adjusts the model to better reflect true ocean conditions (Broquet et al., 2009). The

ROMS/NEMURO model has been used successfully to predict juvenile ocean salmon

growth (Fiechter et al., 2015), explore effects of climate change to ocean ecosystems

(Werner et al., 2007; Kishi et al., 2009, 2010), and examine many other oceanographic

systems (Kishi et al., 2011). This study is the first to use phytoplankton and detritus

concentrations from the ROMS/NEMURO model as covariates in DSCS species

distribution models. These phytoplankton and detritus concentrations serve as estimates

of food availability to DSCS at the depths that they inhabit, which was hypothesized (see

below) to be a critical requirement for their occurrence. This may provide a means to

more accurately predict the location of DSCS occurrences.

Biogeophysical variables (northward and eastward current velocities, temperature,

dissolved oxygen, diatom, and detritus concentrations) were obtained from the

ROMS/NEMURO model. The bottom vertical layer (with a resolution of ∼0.3–8 m off of bottom) was used from the ROMS/NEMURO model output for all variables. Monthly estimates from 1988- 2010 were provided by the models, which were averaged across all months and years, because seasonal averages were collinear with these overall averages. These climatological, multi-year averages were used due to the long-lived nature of DSCS, assuming their persistence is likely due to long-term patterns in availability of food and other habitat variables. The original horizontal resolution of 1/10° (~3 km) was rescaled to match the 30 m resolution provided by the digital elevation model used for bathymetric variables using inverse distance interpolation using R studio (R Core Team 2018).

Bottom currents have been shown to be significant factors in several DSCS habitat suitability models (Davies and Guinotte, 2011; Yesson et al., 2012; Tong et al., 2013) and in particular were found to be significant for *A. dendrochristos* in the Southern California Bight (Huff et al., 2013). Bottom currents are important for delivery of food particles (Davies et al., 2009), preventing smothering of corals with sediment (White et al., 2005), and influencing larval settlement and dispersal. Huff et al. (2013) found that the minimum velocity of January northern currents was positively correlated with *A. dendrochristos* abundance, theoretically due to larval retention in suitable habitats where DSCS already occur.

DSCS subsist on phytoplankton and detritus from primary productivity near the surface (Duineveld et al., 2004; Wagner et al., 2012) and rely on bottom currents to deliver these foods. Diatom, phytoplankton, and zooplankton concentrations were

considered as well as eastern and northern current velocities as covariates for the models (Table 2). This combination of both food abundance and current velocities at depth has been lacking in previous predictive models.

Temperature is an important factor in DSCS habitat as it regulates biological processes and high temperatures can cause coral diseases and mortality (Rogers et al., 2015; Gugliotti et al., 2019). Salinity and temperature have been shown to be important both on the regional (Guinotte and Davies, 2014) and global scale (Yesson et al., 2012). Although temperature was included in this study, salinity was not considered because the range of salinity at which DSCS were surveyed in this study was small (33.06-34.71), similar to Bryan & Metaxas (2006).

Dissolved oxygen (DO) is an important factor in DSCS metabolism and may limit their distribution (Dodds et al., 2007). Deep-sea corals have been observed to process 20-35% of total benthic respiration, which is critical for carbon and nitrogen mineralization (de Froe et al., 2019). DSCS have been shown to have high mortality at low DO concentrations, specifically in waters with less than ~1.5 mL L^{-1} which were shown to be fatal in the Gulf of Mexico (Lunden et al., 2014). DO has been considered in several other DSCS SDMs (Davies et al., 2008; Tittensor et al., 2009; Huff et al., 2013).

DSCS require a hard substrate for attachment and are often found along canyon edges and sloping terrain (Freiwald, 2002). Variations in topographic features are thought to assist in food delivery via current acceleration over bathymetric highs (Dolan et al., 2008), and thus are likely important in DSCS distributions. Bathymetric features such as slope, rugosity, and Bathymetric Position Index (BPI) have been significant variables in

previous DSCS SDMs (Yesson et al., 2012; Tong et al., 2013; Etnoyer et al., 2017). Here, depth, slope, and Bathymetric Position Index (BPI) at two scales were considered for model covariates.

Bathymetric variables (depth, slope, and BPI) were acquired or derived from the 30 m resolution digital elevation model available from the NOAA National Geophysical Data Center (Eakins, 2003). Spatial data manipulation, tabulation, and interpolation was implemented using ESRI™ ArcMAP® v.10. Slope was calculated as the average percent difference between the focal cell and the surrounding 24 cells (n= 3, 90 m radius).

Bathymetric Position Index provides a measure of a location's height relative to the surrounding area, with positive BPI values indicating higher areas and negative BPI values indicating relatively lower areas. This can be useful in DSCS SDMs as DSCS are known to occur in higher locations such as seamounts or ridges (Duineveld et al., 2004; Clark et al., 2006; Tittensor et al., 2009). BPI was calculated by comparing a focal cell's depth value to the mean depth of a surrounding neighborhood of cells. FBPI and BBPI were calculated using an annulus format, such that the mean depth of the surrounding neighborhood was calculated by skipping an inner radius of cells around the focal cell (to avoid cells that are direct neighbors to the focal cell which would skew the mean) and calculating the mean depth for an outer radius of cells (Lundblad et al., 2006). FBPI was calculated using an inner radius of 30 m (n=1) and an outer radius of 240 m (n=8) and the broad scale BBPI was calculated using an inner radius of 300 m (n=10) and an outer radius of 20 km (n=666). These scales were chosen due to their ability to capture

geographic features, such as ridges and troughs at the 240 m scale and seamounts and canyons at the 20 km scale.

Screening of Variables

All variables were assessed for transformation requirements and collinearity. Any variable data with skewed distributions were log-transformed to create a more normal distribution, Pearson's correlation coefficient (r) was used to identify highly correlated variables. Any sets of variables with r>0.7 were deemed collinear and one variable from the set was selected to use in the model selections process.

Maxent Species Distribution Modeling

SDMs of DCSC that use presence-only data is common due to the difficulty and cost of obtaining reliable absence data (Davies and Guinotte, 2011; Yesson et al., 2012). Presence-only data has been utilized in multiple habitat suitability modeling methods including Ecological-Niche Factor Analysis (ENFA) (Bryan and Metaxas, 2007; Dolan et al., 2008), Genetic Algorithm for Rule Set Production modeling (GARP) (Tong et al., 2013), and Maximum Entropy modeling (Maxent) (Phillips et al., 2006; Davies and Guinotte, 2011; Yesson et al., 2012). Maxent is a machine learning technique that has become the preferred method for presence-only SDMs as it has consistently outperformed other methods through model comparison (Wang et al., 2010; Elith et al., 2011). Conceptually, Maxent compares environmental conditions at known location occurrences to randomly selected environmental conditions throughout the study area

(referred to as "background" samples). Maxent fits a probability distribution with "maximum entropy" (i.e. maximum dispersion) for the taxa of interest across a landscape. This maximum entropy probability distribution is constrained by the relationship of the environmental covariates and the taxa's presence data, where a distribution with "higher entropy" is less constrained. For example, a species distribution with "maximum entropy" would have a uniform distribution across all ranges for environmental variables, whereas a species that is constrained by environmental variables that may affect where it is found (such is the case for most species) would have "less entropy".

Performance of maxent models was based on Area Under the receiver operator Curve (AUC) score which is an indicator of how well the model predicts known occurrences. AUC is a discriminatory measure of how well a model predicts known presences and absences across all possible thresholds, and reports this as a score ranging from 0 to 1 (Fielding and Bell, 1997). In Maxent, AUC scores are calculated by comparing predictions at known presences to the proportion of background points predicted as presences (Phillips et al., 2006). A Maxent model with an AUC score of 0.5 is considered to predict presences no better than chance, and a score of 1 signifies all presences were predicted correctly (Phillips et al., 2006). Ten percent of the known occurrences were withheld from the model to use as test data, and AUC values for this test data were used for reporting.

Confidence intervals were created by bootstrapping 100 samples for all models, and variable importance was assessed using Maxent's Percent Contribution output.

Percent variable contribution was calculated by tracking gains to the penalized average

log likelihood in each iteration of Maxent's algorithm (Elith et al., 2011). In addition to

percent contribution, each variable was separately permuted to assess the effect of that

individual variable on the model. Permutation importance is calculated by randomly

permuting presence and background for each variable in turn, and the resulting gain or

loss to training AUC is tallied (Elith et al., 2011). A large decrease in training AUC

would indicate that the variable in turn is important to the model (Elith et al., 2011). In

addition to full models, single variable models were run to elucidate which variables are

strong drivers in the full model. Varying levels of beta multipliers were tested for each

model to determine the best constraints on variables as suggested by Warren and Seifert

(2011). A larger beta multiplier value will have a more restricted range in variable values

that are considered suitable habitat for the species (Warren and Seifert, 2011). Four beta

values (0.5, 1, 2, 3) similar to those tested by Warren and Seifert (2011) were tested and

ranked by Akaike's Information Criteria corrected for small sample size (AICc). The

most parsimonious Maxent model was then used to make predictions for the SCB.

Maxent models were developed using the 'dismo' package in R (Hijmans et al., 2017; R

Core Team, 2019).

Generalized Additive Models

When absence data is available and reliable, Generalized Additive Models

(GAM) are a preferred method to predict taxa presence/absence or density (Elith et al.,

2011; Huff et al., 2013; Ross and Howell, 2013; Winship et al., 2020, 2020). GAMs are

generalizations of multiple linear regressions that can fit non-linear relationships between a dependent variable and multiple predictors in the same model (Zuur et al., 2009). Non-linear relationships between a variable and a response are fit using a process known as "smoothing", where unique equations are fit for windows of the variable range (Wood et al., 2016). GAMs have predicted known presences and absences well in other SDMs (Suárez-Seoane et al., 2002; Drexler and Ainsworth, 2013; Grüss et al., 2014).

GAMs were fit using an Integrated Nested Laplace Approximation (INLA) Bayesian approach due to its high processing speed and its reliable results (Rue et al., 2009; Held et al., 2010; Zuur et al., 2017). Individual parameter estimates and their associated credible intervals (CrI) are approximated by taking integrals of the posterior joint distribution of the model (which includes all model parameter values) (Zuur et al., 2017). A CrI is similar to the frequentist confidence interval in that a parameter whose CrI contains zero is not considered to be important in the model (Zuur et al., 2017). Preliminary frequentist GAMs that included a spatial error structure were fit using the 'mgcv' package in R (Wood, 2019), however extended fit times (>15 hours) restricted the ability to perform model validation in a reasonable amount of time. This was the motivating factor for using the INLA approach. The modeling approach, model selection procedure, and all the code to fit the GAMs for this part of the project was developed by Mark Henderson, using the 'R-INLA package' (Lindgren and Rue, 2015).

Models that include geographic data can often contain a form of pseudoreplication known as Spatial Autocorrelation (SAC), which can be addressed by adding a spatial dependency covariance structure (Zuur et al., 2017). Spatial

autocorrelation occurs when dependence exists between nearby sampling locations

because locations near one another experience similar conditions, and this dependency

can be observed as spatial patterns in the residuals (Zuur et al., 2009, 2017). Models that

have SAC may underestimate prediction errors and have poor prediction accuracy

(Gelfand et al., 2006), thus it is important to consider options that account for SAC. To

reduce SAC in the model, R-INLA utilizes the Matérn correlation function to estimate a

spatial covariance matrix (Zuur et al., 2017). The Matérn correlation function contains an

unknown parameter, kappa, which is the range at which spatial dependency occurs; for

larger values of kappa, the smaller the distance at which dependency occurs (Zuur et al.,

2017). R-INLA uses a Stochastic Partial Differential Equation (SPDE) to solve for this

unknown range parameter as well as the unknown variance parameter as outlined in Zuur

et al. (2017).

To find the most parsimonious model with the best fit to the data, the R-INLA

code included a model selection process aimed to assess (1) whether including a spatial

dependency structure improved the model, and (2) which variables have a non-linear

relationship with the response and should be smoothed. First, a global model with all

noncollinear variables as linear terms (i.e. a Generalized Linear Model) was compared to

a spatial global model, which was the same model with a spatial dependency structure.

WAIC (Watanabe-Akaike Information Criteria) was used to determine whether to move

forward with the spatial or non-spatial model. WAIC consists of two terms representing

model fit and complexity (Watanabe, 2010), and is an improvement on other Bayesian

model selection criteria (such as the Deviance Information Criterion) (Gelman et al.,

2013). For every model we also calculated the ΔWAIC, which was the difference

between a given model and the model with the lowest WAIC. The model with fewest

linear covariates, and knots from smoothed parameters, with a ΔWAIC of less than 5 was

selected as the most parsimonious model to use for the analysis. Second, to reduce the

total number of models tested in the model selection process, a two-stage process was

carried out to determine which variables should be modeled using a smoothed

relationship instead of a linear relationship. The first stage determined which of the four

bathymetric variables (depth, slope, BBPI, and FBPI) should be smoothed. All

biogeophysical variables (eastern currents, northern currents, food supply, temperature,

and dissolved oxygen) were held linear during this stage. All combinations of smoothed

and linear bathymetric variables were tested (e.g. the first model included depth as a

smoothed term and all other variables were held linear, the second model included depth

and slope as smoothed terms and the remaining variables were held linear, etc; see Table

A1 for specific models tested). The model with the lowest ΔWAIC score was chosen and

whichever variables were selected to be smoothed from this stage were held smoothed in

the second stage. The second stage involved repeating the same process for

biogeophysical variables (currents and diatom concentrations). During this second stage,

northern and eastern currents were tested as either stand-along smoother or linear

variables, or as a tensor to account for the combined effects of the directional currents

(see Table A2 for examples of specific models tested). The number of knots used for each

variable during the smoother selection test was predetermined based on a non-spatial,

frequentist GAM fit using the 'mgcv' package (Wood, 2019). The area surveyed within

each cell was used as an offset in all models. An offset is a known additive term (Zuur et al., 2009) that when applied in this manner can account for some of the bias of uneven survey areas across cells. This process was used for each taxa, and results from the final models were used to create response plots for each variable (all other variables were held at their mean) and to generate predictive species distribution maps for the SCB.

Model uncertainty in the form of CrI range can provide information on the confidence of model estimates. I explored model uncertainty by inspecting the CrI range for predictions. Predictions of the probability of a species occurrence were made using the lower (5%) and upper (95%) credible interval, and the difference between the two was used to determine high levels of uncertainty. A credible interval range greater than 0.25 probability for any location within the SCB was considered as having high uncertainty, and areas with this high uncertainty were masked in predictive maps to prevent the visualization of DSCS probabilities that were highly uncertain.

The importance of model variables included for each taxa was assessed using 10-fold cross-validation. Cross-validation was used to determine how often variables were selected as important (i.e. if it was selected as a smoothed variable or was a linear variable without zero in the CrI) in the final model and to determine how well the model preformed via AUC score. Ten percent of the model data was randomly selected and set aside as test data, while the remaining 90 percent was used to build a model using the steps described above. This was repeated 100 times and the results were summarized as how often each variable was important in the model (reported as a percent), and I also

tabulated the average WAIC scores for the global non-spatial model, global spatial

model, and final model, as well as the test and training AUC scores.

Suitable Habitat Within CINMS Waters

To provide information on the extent of protected areas for highly suitable DSCS

habitat within the Channel Islands National Marine Sanctuary (CINMS), predicted areas

of suitable habitat both inside and outside the sanctuary were quantified. To do this,

threshold values were created such that only areas above a specific value were considered

suitable habitat. Two thresholds were used to consider areas of broadly suitable habitat:

(1) a threshold of 0.5 habitat suitability (based on Maxent's logistic output) or 0.5

probability (based on the GAM's probability of presence) indicated generally good) and

areas of more restricted suitable habitat; and (2) a threshold of 0.75 habitat suitability or

probability of presence indicated more restricted areas of better habitat. These threshold

values were chosen to replicate the process done previously for determining the area of

protected coral and sponge habitat along the west coast, including the SCB, by Guinotte

& Davies (2014). This method is not ideal as threshold values may lack an ecological

basis (Osborne et al., 2001), but it provides a rough estimation of where hot spots may

occur. Maxent output provides information on the suitability of one area compared to

another, and thus prediction values are somewhat arbitrary (Osborne et al., 2001).

Probability of presence provides a more straightforward comparison between predicted

cell values; thus a 0.5 threshold will represent a 50% probability of presence. All model

predictions were mapped using ESRI™ ArcMAP® v.10 using a 240 m x 240 m

resolution fit to the extent of the SCB within 50 to 500 m depth. To calculate the total

area for each threshold, prediction outputs were masked to only depict values greater than

the given threshold, then the total number of cells not masked were multiplied by the area

of the individual cells (0.0069 km^2). These remaining areas were then compared to the

total area of the SCB between 50 – 500 m and the total area in the CINMS between 50 –

500 m, both of which were reported as a percent. Additionally, the areas of high

suitability with the CINMS were compared to the area of high suitability across the SCB,

which was also reported as a percent.

RESULTS

Species Occurrences

Line transects were conducted by submersible in 8415 cells (30 m x 30 m) within

the SCB to assess the presence of the three DSCS taxa (*A. dendrochristos*, *P. longispina*,

and Porifera sp. To put this in perspective, this means that of the 44 million 30 x 30 m

cells in the SCB between 50 – 500 m, we surveyed only 0.0002% of them. The removal

of deeper dives resulted in the loss of less than 3% of occurrences for each species (0.1%,

0.3, and 2.4% of taxa occurrences for *A. dendrochristos*, *P. longispina*, and Porifera sp.,

respectively). For the observations between 50-500m, Porifera sp. had the highest

number of occurrences (n= 1403 cells), while *A. dendrochristos* (n=674 cells) and *P.*

longispina (n=606 cells) had fewer. These observations occurred mostly south of Santa

Cruz, San Clemente, and San Nicholas Islands, north of Santa Barbara Island, and along

the coast (Figures 2, 3, & 4).
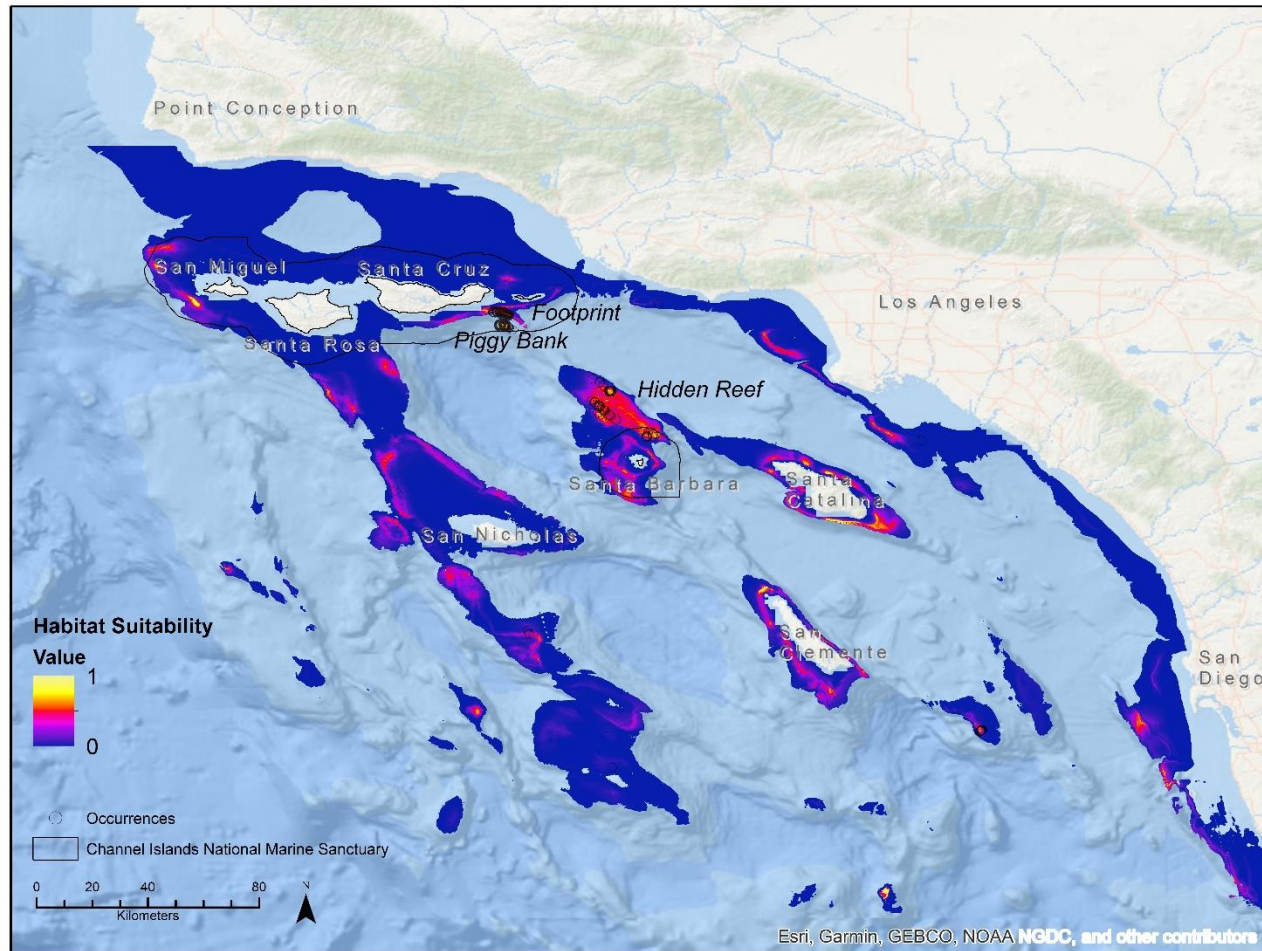
Figure 2. Maxent model predictions for *Antipathes dendrochristos* (n=674) in the Southern California Bight. Model predictions used a beta multiplier of 0.5.
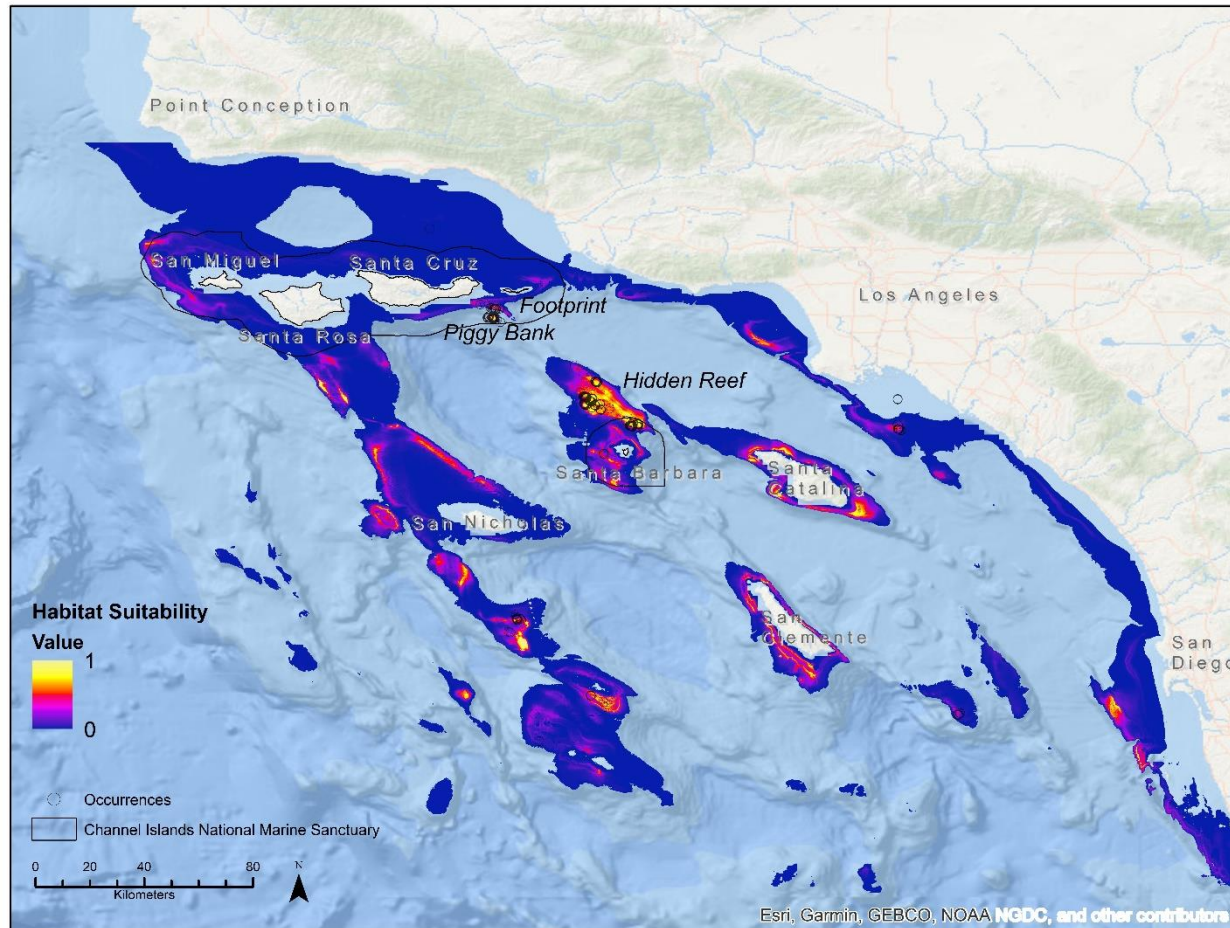
Figure 3. Maxent model predictions for *Plumarella longispina* (n=606) in the Southern California Bight. Model predictions used a beta multiplier of 0.5.
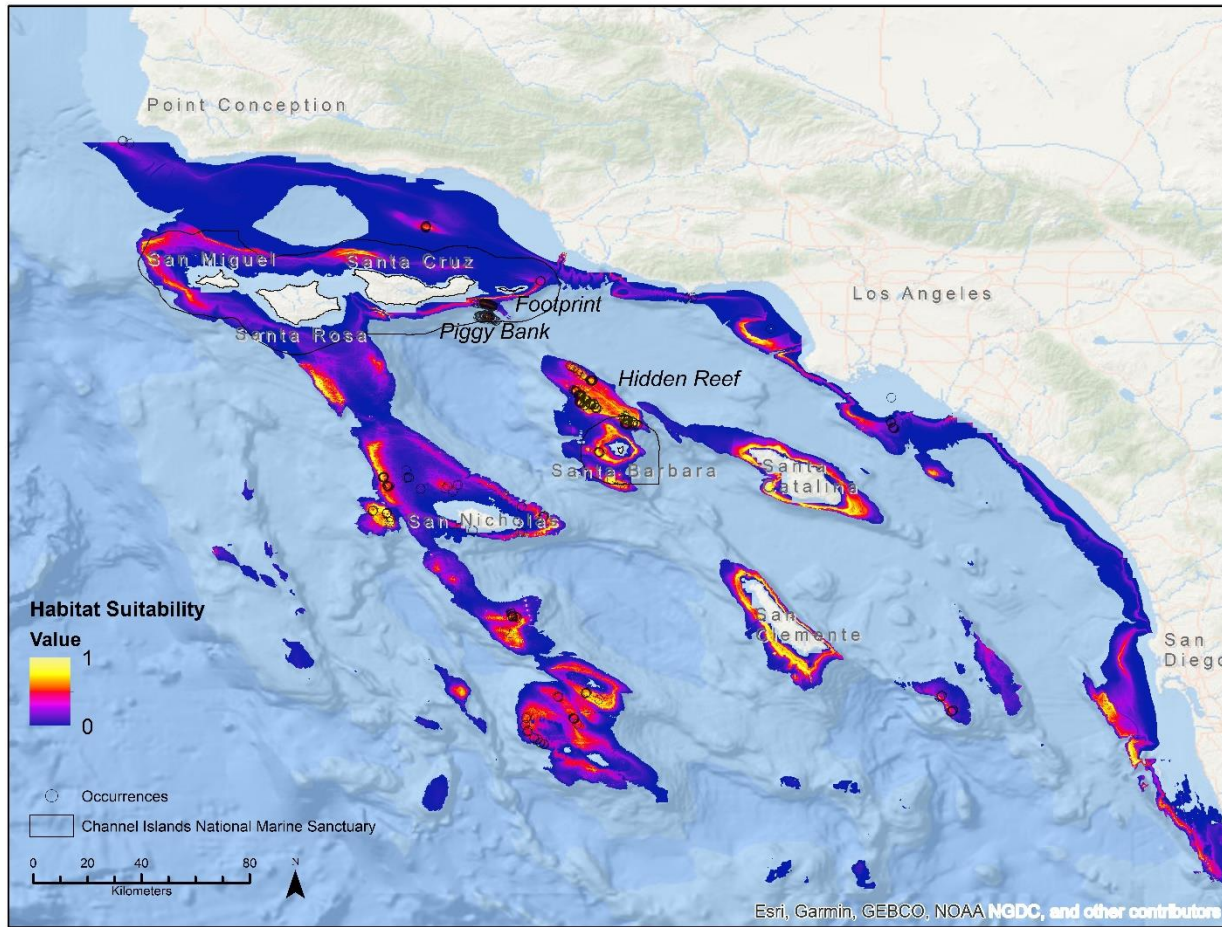
Figure 4. Maxent model predictions for Porifera sp (n=1403) in the Southern California Bight. Model predictions used a beta multiplier of 0.5.

Environmental Variables

Seven of the original ten covariates were used for model fitting after elimination based on collinearity (Table 2). The final set of covariates used for model testing included (1) northward bottom currents, (2) eastward bottom currents, (3) average diatom concentration, (4) depth, (5) slope, (6) broad scale Bathymetric Position Index (BBPI) and (7) fine scale Bathymetric Position Index (FBPI). Diatom concentration, phytoplankton, zooplankton, detritus, temperature, and DO were all strongly correlated (Pearson's correlation coefficient of 0.9 or above); therefore, diatom concentration was considered representative of all the collinear covariates, and the other covariates were excluded from consideration to avoid redundancy among variables.

Maxent Results

The best model for all three taxa used a beta multiplier of 0.5 (Table 3) and had average test AUC values of 0.916 (*A. dendrochristos*), 0.919 (*P. longispina*), and 0.831 (Porifera sp.). Results for all three taxa were generally similar, specifically in terms of variable contributions. Diatom concentration, BBPI, and depth were the greatest contributing variables for all models in this rank order, except for the sponge (with a ranking of Depth, Diatom, and BBPI) (Table 4).

Table 3. Beta multiplier selection table for *A. dendrochristos, P. longispina, and* Porifera sp.. All four models include northward and
eastward bottom currents, diatom concentration available at depth, depth, broad scale Bathymetric Position Index, and fine scale Bathymetric
Position Index as variables.

Taxa	Beta Multiplier	No. of Parameters	AICc	dAICc
A. dendrochristos	0.5	116	41210.7	0
A. dendrochristos	1	121	41878.3	667.6
A. dendrochristos	2	93	42631.6	1420.9
A. dendrochristos	3	78	43154.1	1943.4
P. longispina	0.5	68	6158.5	0
P. longispina	1	36	6169.5	11
P. longispina	2	28	6333.5	175
P. longispina	3	18	6405.8	247.3
Porifera sp.	0.5	148	102923.3	0
Porifera sp.	1	121	103647.8	724.5
Porifera sp.	2	116	104578.7	1655.4
Porifera sp.	3	18	105123.4	2200.1

Table 4. Maxent variable contributions for *Antipathes dendrochristos*, *Plumarella longispina*, and Porifera sp.. Percent contribution is estimated by the increase in regularized gain for each training iteration. Permutation importance is percent change to the original AUC when the variable values are randomly permuted. Values above 20% Percent Contribution are highlighted in bold.

	Antipathes dendrochristos	*Antipathes dendrochristos*	*Plumarella longispina*	*Plumarella longispina*	Porifera sp.	Porifera sp.
Variable	Percent	Permutation	Percent	Permutation	Percent	Permutation
Depth	**21.3**	**22.9**	**19.2**	**62.3**	**40.2**	**32.2**
BBPI	**28.8**	**41.7**	**25.9**	**12**	**23.9**	**25.6**
FBPI	0.5	0.1	9.6	0.9	0.6	0.8
Slope	12.6	0.6	9.3	1.9	2.8	3.4
Diatom	**30.8**	**25.5**	**28.7**	**14.2**	**27.7**	**31.5**
Northern Current	5.3	8.8	4.5	6.3	3.4	3.9
Eastern Current Velocity	0.8	0.4	2.8	2.3	1.4	2.6

BBPI was the highest contributor for *A. dendrochristos* and *P. longispina*, and the second highest contributor for Porifera sp. (36.9%, 33.2%, and 33.6% respectively, Table 4). Habitat suitability had an increasing trend with respect to BBPI for all three taxa, and suitability was low for negative values of BBPI (Figure 5). *A. dendrochristos* reached peak suitability of 1 around a BBPI value of 800. Both *P. longispina* and Porifera sp. reached a peak habitat suitability just below 1 around a BBPI value of 1000 (Figure 5).
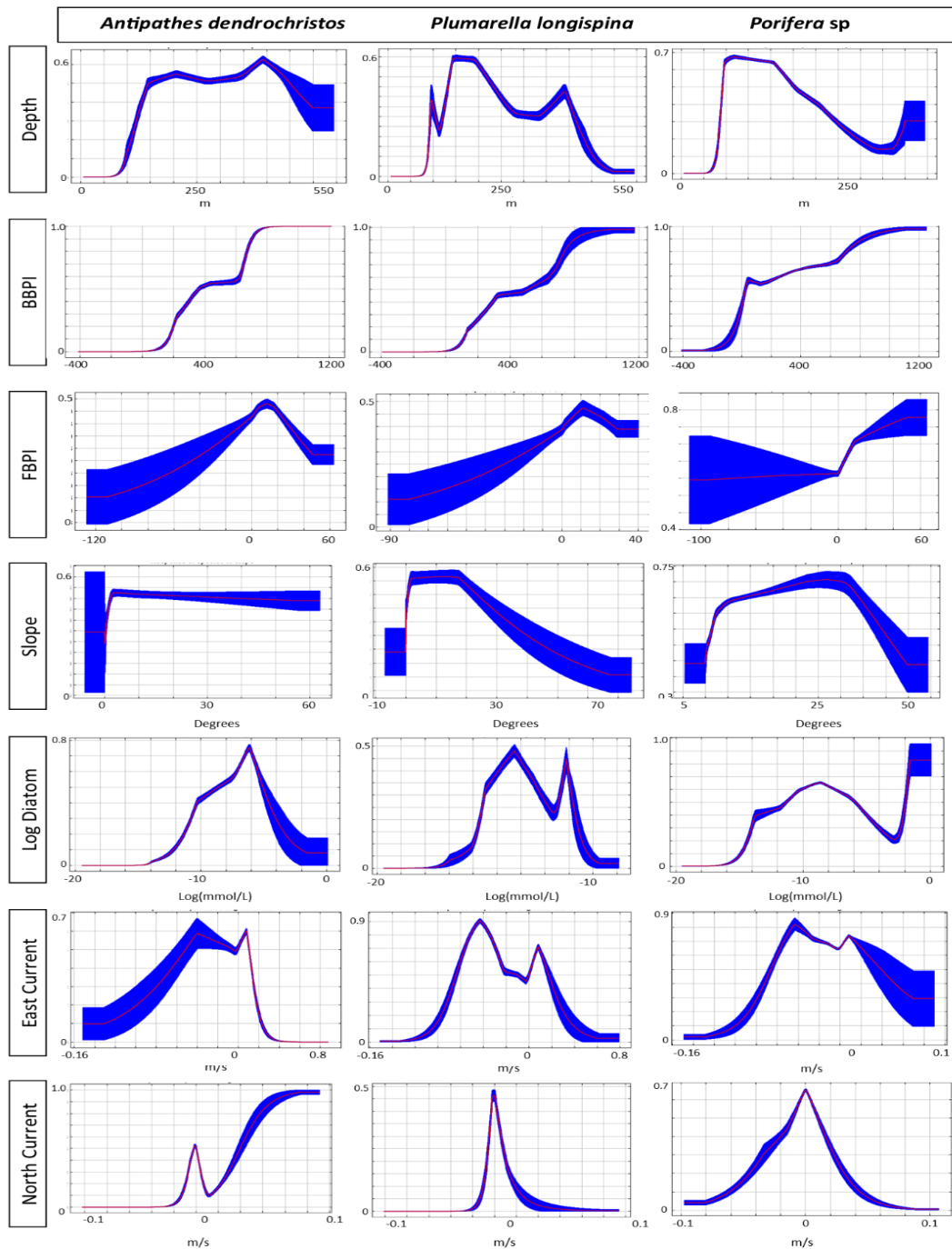
Figure 5. Response plots for *Antipathes dendrochristos*, *Plumarella longispina*, and Porifera sp. full maxent models. All models were made with a beta multiplier value of 0.5 and bootstrapped with 100 samples. Y axis for all plots is habitat suitability.

Diatom concentration was the second highest contributing variable for *A. dendrochristos* and *P. longispina*, and was the third highest contributor for Porifera sp. (contributing 23.0%, 26.8%, and 19.8%, respectively), with relatively high permutation importance compared to other variables (Table 4). Highest habitat suitability occurred at low diatom concentrations close to zero (<0.001mmol/L when log of diatom concentration was backtransformed to raw values) (Figure 5). *A. dendrochristos* had a peak habitat suitability of 0.8 that occurred around 1e-6 mmol/L, while *P. longispina*'s highest habitat suitability of 0.5 occurred at a lower concentrations around 1e-9 mmol/L, but had a generally wider range of higher habitat suitability (>0.2) between the ranges of 1e-11 to 1e-4 mmol/L. Porifera sp. had an even wider range of higher suitability levels (>0.2) between 1e-14 and 1e-3 mmol/L, with a peak habitat suitability around 1e-6 mmol/L (Figure 5).

Depth was the highest contributor to the model for Porifera sp. and the third highest contributor for *A. dendrochristos* and *P. longispina* (33.9%, 14.9%, and 22.3% respectively, Table 4). It also had relatively high permutation importance for all three taxa (Table 4). Depth had a wide range of higher suitability (>0.5) between 150-450 m for *A. dendrochristos* with peak suitability of 0.6 occurring just below 400 m (Figure 5). Habitat suitability peaked just below 0.6 around 150 m depth for *P. longispina* but had a range of habitat suitability >0.3 between ~100-400 m (Figure 5). Porifera sp. peaked just below 0.7 habitat suitability around 100 m depths with a steady decline in habitat suitability in deeper waters (Figure 5).

Slope was the fourth highest contributing variable for *A. dendrochristos,* the fifth highest for Porifera sp., and the sixth highest contributor for *P. longispina* (Table 4). Slope had a relatively flat trend for *A. dendrochristos*, slightly decreasing in habitat suitability from just above 0.5 to just below 0.5 for the majority of the range of slope values (Figure 5). *P. longispina* had the highest habitat suitability just above 0.45 between 0° and 20° slope, then steadily decreased for all higher values of slope (Figure 5). Porifera sp. had a dome-shaped response plot; when slope was 10° the habitat suitability slowly increased to a peak suitability of ~0.7 around a slope of 25°, and then suitability quickly declined between slope of 25° and 45° (Figure 5).

Northern current was the fourth highest contributor for *P. longispina* and Porifera sp., and the fifth highest contributor for *A. dendrochristos* (Table 4). Response plots for northern currents had sharp peaks with highest suitability between 0.5-0.6 occurring at velocities near zero for both *P. longispina* and Porifera sp. (Figure 5). *A. dendrochristos* had a small peak around 0 m/s, but reached maximum habitat suitability of 1 at relatively higher current velocities (~0.08 m/s). Eastern currents contributed relatively low amounts to the three models, between 1.3-4% (Table 4). Porifera sp. and *P. longispina* had peak habitat suitability between 0.8-0.9 just above 0.04 m/s in the westward current direction (indicated by negative values for eastern currents, Figure 5), although both had relatively high (>0.5) habitat suitability values in both low eastern and western directions (Figure 5). *A. dendrochristos* had peak habitat suitability just above 0.6 at relatively low eastern

current velocity (<0.02 m/s), although it also had high suitability around 0.04 m/s in the western direction, similar to *P. longispina* and Porifera sp. (Figure 5).

FBPI was the lowest contributing variable for all three taxa (0.7-1.1%, Table 4). *A. dendrochristos* and *P. longispina* had an increasing trend for FBPI with peak habitat suitability around 20, which then decreased for higher FBPI values, particularly for *A. dendrochristos* (Figure 5). Porifera sp. had peak habitat suitability just above 0.7 around a FBPI value of 10. Porifera sp. had a generally increasing trend with peak habitat suitability around an FBPI value of 50 (Figure 5).

Single variable response plots were broadly consistent with full model response plot for depth, FBPI, northern currents, slope, and diatom concentration (Figure A1). The shape of BBPI changed the most, displaying a distinct peak for all three taxa (Figure A1). Eastern currents were still peaked but were broader in range (Figure A1). Slope for *A. dendrochristos* was mostly flat in the full model, but was dome-shaped and more similar to the other two taxa in the singe variable models (Figure A1).

A. dendrochristos, P. longispina, and Porifera sp. suitable habitat was predicted across the SCB, and there was a large amount of similarity across the three taxa (Figures 2, 3, & 4). The highest suitability areas were found on: the western and southeastern side of the northern section of CINMS, throughout the southern section of CINMS (around Santa Barbara Island), ringing the southern Channel Islands (Santa Catalina, San Clemente, and San Nicholas), north of Santa Barbara Island at Hidden Reef, and along parts of the southern coast near San Diego (Figures 2, 3, & 4). Species occurrences appear in high

suitability areas in the north, with many high suitability areas that do not have occurrence data (Figures 2, 3, & 4). The largest hot spot for *A. dendrochristos* is at Hidden Reef north of Santa Barbara Island (Figure 2). *P. longispina* had similar geographic trends to *A. dendrochristos* predictions (Figure 2), but slightly more expansive. The largest hot spots for *P. longispina* and Porifera sp. were at Hidden Reef north of Santa Barbara Island (Figures 3 & 4), similar to *A. dendrochristos*. Porifera sp. had very similar geographic trends to *A. dendrochristos* and *P. longispina*, but was more extensive.

GAM Results

A spatial random effect was included in the best GAMs for all each of the three taxa. For all three taxa, models without the spatial random effect showed patterns of SAC in the residuals in that a majority of the residuals were negative with positive residuals occurring in more eastern areas (Figures A12, A13, & A14) and had much higher WAIC scores (ΔWAIC scores of 8531.8 for *A. dendrochristos*, and 10337.0 for *P. longispina,* and 7300.9 for Porifera sp., Table 5), strongly supporting the inclusion of the spatial random effects. Some SAC patterns persisted after including a spatial random effect, specifically clusters of small negative residuals throughout the study area, but these clusters diminished compared to the non-spatial model (Figures A12, A13, & A14).

Table 5. Maxent variable contributions for *Antipathes dendrochristos*, *Plumarella longispina*, and Porifera sp.. Percent contribution is
      estimated by increase in regularized gain for each training iteration. Top three contribution covariates values are in bold for each species.

Taxa	Model	WAIC	ΔWAIC	Test AUC	Train AUC
A. dendrochristos	Global GLM	10790.2	8531.8	-	-
A. dendrochristos	Global GLMM	2526.2	267.8	-	-
A. dendrochristos	Final GAMM	2258.4	0	0.86	0.95
A. dendrochristos	Maxent	-	-		0.916
P. longispina	Global GLM	12524.2	10337.0	-	-
P. longispina	Global GLMM	2647.1	459.9	-	-
P. longispina	Final GAMM	2187.2	0	0.75	0.95
P. longispina	Maxent	-	-		0.919
Porifera sp.	Global GLM	11847.3	7300.9	-	-
Porifera sp.	Global GLMM	5151.3	604.9	-	-
Porifera sp.	Final GAMM	4546.4	0	0.59	0.89
Porifera sp.	Maxent	-	-		0.831

Depth, slope, northern currents, and eastern currents were all important variables (i.e. they did not include zero in their CrI) in the final models for all three DSCS. Probability of occurrence showed more complex relationships with depth and currents while relationships with slope were generally flat, based on the response plots for the covariates (Figure 6). Diatom concentration was not important in any of the three GAMs, and probability of occurrence was generally flat across the range of diatom values for all three taxa (Figure 6). While some similarities occurred across taxa, variation was also present in both the overall trend and the variables that were important for the model.
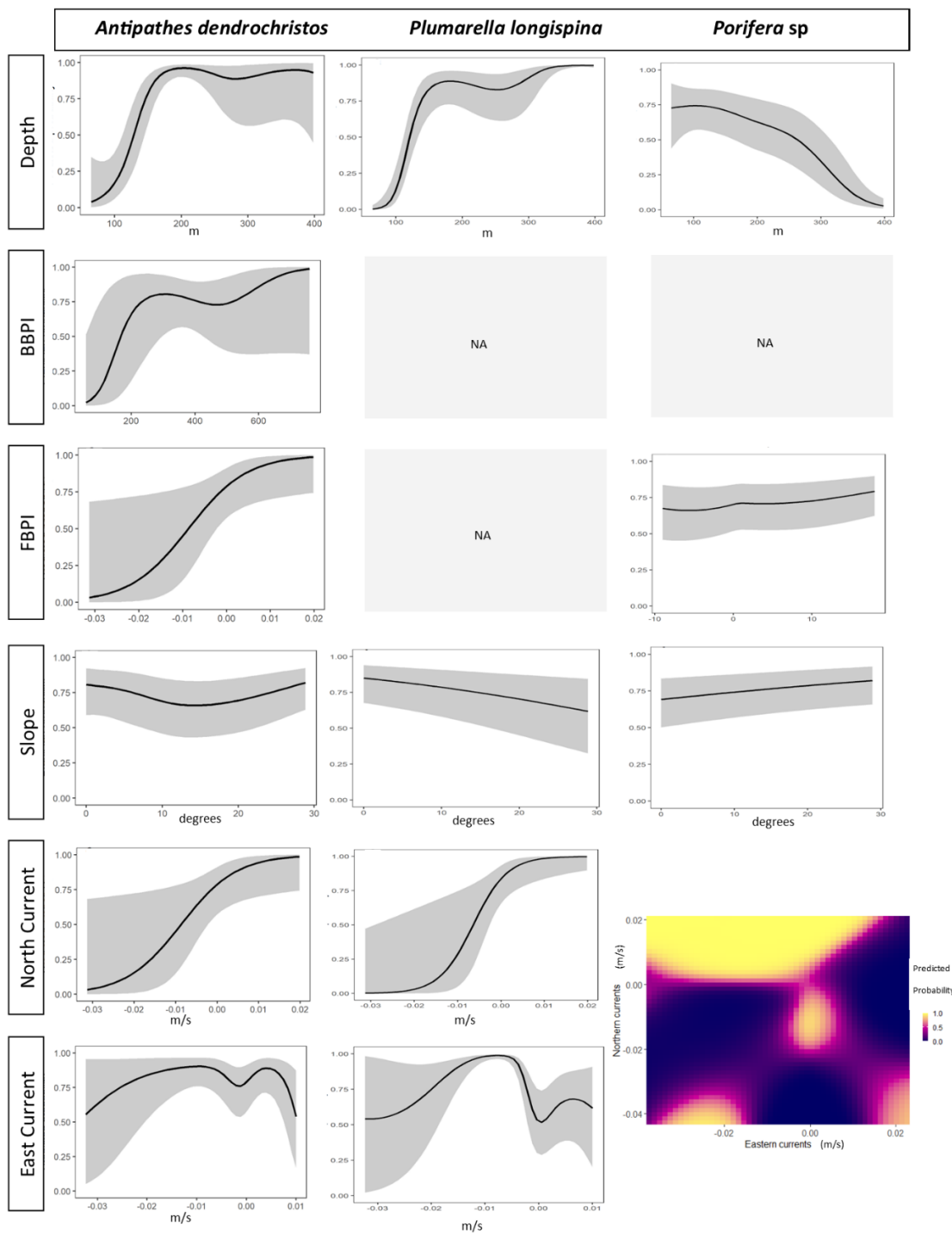
Figure 6. Response plots for predicted probability of occurrence for *Antipathes dendrochristos*, *Plumarella longispina*, and Porifera sp. GAMs. "NA represents variables that were not important.

Depth was important in all three models (Table 6) and showed a strong relationship with probability of presence (Figure 6). *A. dendrochristos* had a steeply increasing response curve for depth, where peak probability of presence (>0.75) occurred at depths around 150 m and stayed consistently high for all deeper depths, although with a wider range of certainty for depths greater than ~250 m. Probability of *P. longispina* had a similar pattern, with an increasing trend from 0 to 75 m, then a mostly consistent trend with peak probability of ~1 near 300 m (Figure 6). Probability of Porifera sp. had an inverse relationship with depth, where greater probabilities occurred in shallower waters and decreased gradually with increased depth, with maximum probability of occurrence around 100 m (Figure 6).

Table 6. Final variables for best GAM models for *Antipathes dendrochristos*, *Plumarella longispina*, and Porifera sp.. Smoothed variables are represented by s(variable) and a tensor is represented by te(variable 1 x variable 2).

Species	Predictors
Porifera *sp.*	s(Depth)
	Slope
	s(FBPI)
	te(N Current x E Current)
P. longispina	s(Depth)
	Slope
	s(E Current)
	s(N Current)
A. dendrochristos	s(Depth)
	s(Slope)
	s(BBPI)
	s(FBPI)
	s(E Current)
	s(N Current)

Other bathymetric variables were less important in the GAMs for the three DSCS

taxa. BBPI was only important in the *A. dendrochristos* final model (Table 5). The

probability of *A. dendrochristos* presence was high (~0.75) with BBPI values greater than

200, although uncertainty around these values were quite wide (Figure 6). FBPI was

important in *A. dendrochristos* and Porifera sp. final models (Table 5). Probability of

presence for *A. dendrochristos* had a sigmoidal relationship with FBPI*,* but it had a wide

CrI (Figure 6). The relationship between FBPI and probability was relatively flat for

Porifera sp. (Figure 6). Slope was important in all three models (Table 5), but did not

appear to have as large an effect on the probability of occurrence as some of the other

covariates, since the relationship was relatively flat for all species (Figure 6). *P.*

longispina showed a slight negative trend, Porifera sp. showed a slight positive trend, and

A. dendrochristos had a slightly concave shape, but the probability changed no more than

0.1-0.2 for any of these trends (Figure 6).

Eastern current was also important in all final models (Table 5) and had strong

relationship with all three taxa (Figure 6). High probability of *A. dendrochristos* (>0.5)

occurred across the range of eastern and western velocities, with peak probabilities at

relatively weak velocities in both the eastern and western direction, although a fair

amount of uncertainty occurred for the majority of the current range in the western

direction (Figure 6). Probability of *P. longispina* peaked at relatively weak velocities in

the western direction, with widespread uncertainty for stronger western currents and a

fair amount of uncertainty for eastern currents (Figure 6). The best Porifera sp. model

included a tensor for eastern and northern currents, with peak probability occurring in northern and western currents (Figure 6). High probability of Porifera sp. occurrence occurred near zero m/s in the eastern current direction and relatively weak velocity in the southern direction (Figure 6).

Northern currents were also important in all three models, with generally higher probability occurring in northern current velocities (Figure 6). Probability of *A. dendrochristos* and *P. longispina* had a sigmoidal relationship with northern currents, with low probability of occurrence in southern currents and high probability of occurrence occurs in northern currents, although uncertainty in southern currents was much greater than in northern currents (Figure 6).

Cross validation revealed northern and eastern currents, and FBPI were generally important predictors in 100 cross-validation models, depending on taxa (Table 7). *A. dendrochristos* cross-validation models had depth and FBPI as important variables all models, with slope and eastern currents in over 80% of all models (Table 7). AUC was relatively high for both training and test data (0.949 and 0.826, respectively, Table 7). *P. longispina* had northern and eastern currents as important variables in all models, depth in over half of the models, and also had a high AUC for both training and test data (0.947 and 0.729, respectively, Table 7). Depth, FBPI, and northern and eastern currents were important in all Porifera sp. cross validation models, slope was important in over half of all models, and had a good training AUC (0.6892) but a poor test AUC (0.602) (Table 7).

Table 7. Cross validation results for *Antipathes dendrochristos*, *Plumarella longispina*, and Porifera sp.. WAIC and AUC scores area averaged across 50 cross validation runs. Variable percent are the number of times a variable either 1) is a linear predictor and does not include zero in the 90% CrI or 2) performed better in the model as a smoothed variable.

	A. dendrochristos	*P. longispina*	Porifera sp.
Non Spatial Global Model WAIC	10809.6	11280.7	10669.7
Spatial Global Model WAIC	2588.9	2362.5	4651.2
Final Spatial Model WAIC	2300.2	2214.0	4570.2
Train.AUC	0.949	0.947	0.892
Test.AUC	0.826	0.729	0.602
Depth	100.0%	66.7%	100.0%
BBPI	33.3%	41.7%	33.3%
FBPI	100.0%	33.3%	100.0%
Slope	83.3%	25.0%	66.7%
Diatom Concentration	41.7%	25.0%	16.7%
Northern Current	33.3%	100.0%	100.0%
Eastern Current	83.3%	100.0%	100.0%

The majority of low uncertainty, high probability predictions for all three GAMs were found in patches throughout the Channel Islands, on ridges between islands, and in select areas along the coast (Figures 7, 8, and 9). *A. dendrochristos* had concentrated areas of high probability of occurrence along the western portion of the northern section of CINMS near San Miguel, on the eastern and southern side of Sant Cruz Island, along the bathymetric contours around San Nicholas Island, ringing Santa Catalina, Santa Barbara, and San Clemente Islands, and regions surrounding Santa Barbara Island, including to the north at Hidden Reef (Figure 7). Peaks of bathymetric features in the southern portion of the SCB were also hot spots for *A. dendrochistos* as well all near the coast of San Diego (Figure 7).

Figure 7. GAM model predictions for *Antipathes dendrochristos* (n= 674) in the Southern California Bight. The best model included depth, slope, BBPI, FBPI, eastern currents, and northern currents as predictive variables and a spatial random effect. Lower plot excludes areas where predictions had a high degree of uncertainty (i.e., plot shows areas with credible interval ranges less than 0.25 probability). Broad areas with smaller ranges of uncertainty include the majority of the Santa Barbara Basin, east of San Miguel Island, along the coast.

Figure 8. GAM model predictions for *P. longispina* (n=606) in the Southern California Bight. The best model included depth, slope, eastern currents, and northern currents as predictive variables and a spatial random effect. Lower plot excludes areas where predictions had a high degree of uncertainty.
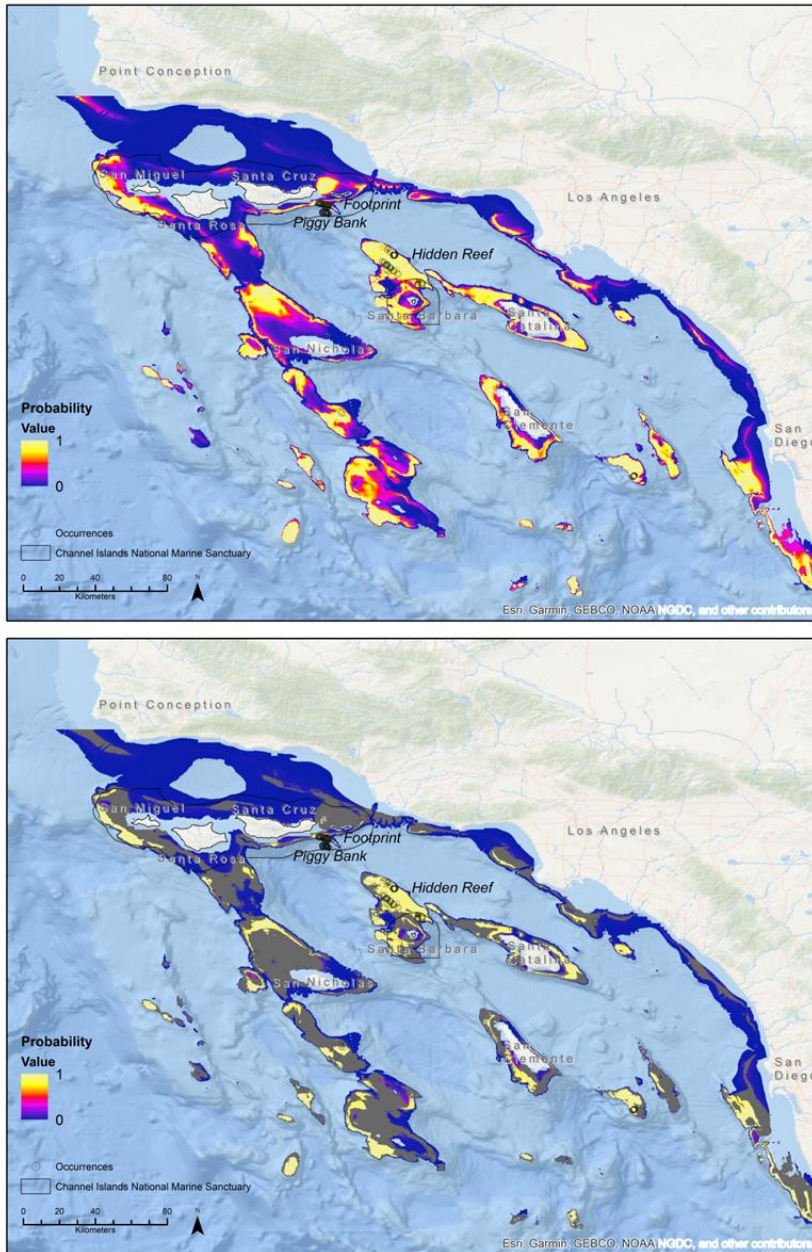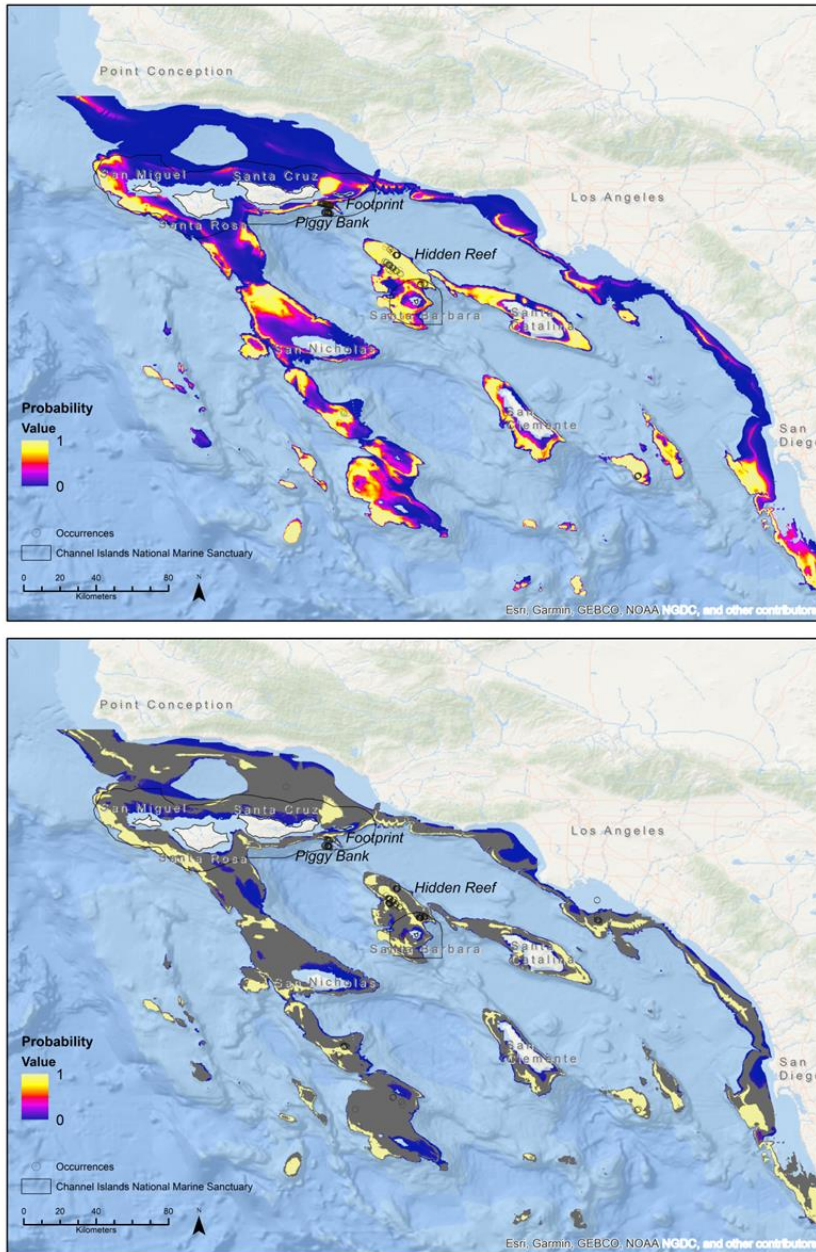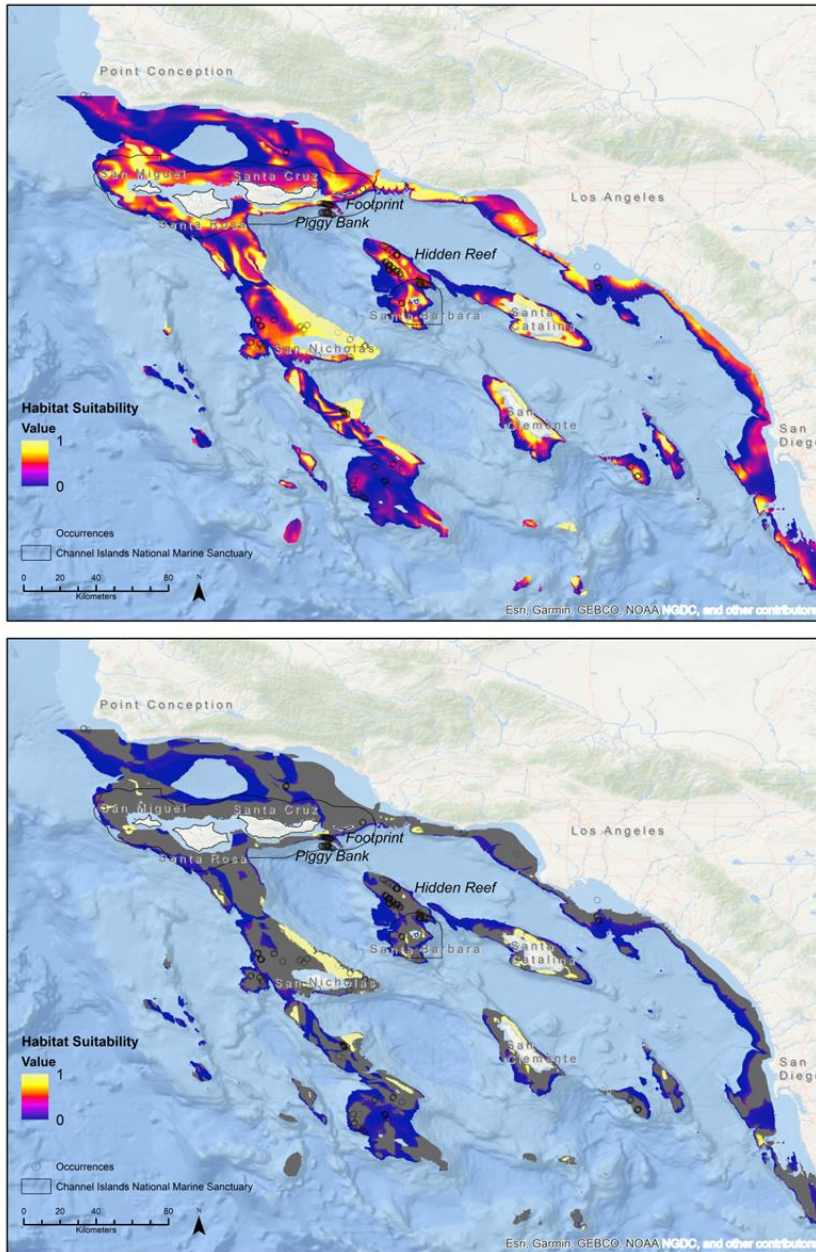
Figure 9. GAM model predictions for Porifera sp (n=1403) in the Southern California Bight. The best model included depth, slope, FBPI, and a tensor between eastern, and northern currents as predictive variables and a spatial random effect. Lower plot excludes areas where predictions had a high degree of uncertainty.

P. longispina had a wide predicted distribution, with high areas of high probability throughout the SCB (Figure 8). Large areas of high probability occurred throughout the Santa Barbara Channel, ringing the northern and southern islands, and through the channel east of Santa Cruz Island (Figure 8). Hidden Reef had a mix of high and mid-range probabilities, as did the banks south of San Nicholas Island (Figure 8). High probability also occurred on the peaks of the bathymetric features in the southern portion of the SCB (Figure 8).

Porifera sp. had concentrated hot spots of high probability and a wide distribution of mid-range probabilities throughout the SCB, with similar trends of higher probability ringing the islands and other select locations (Figure 9). Hot spots occurred on the northern side of San Miguel and Santa Rosa, and Santa Cruz Island, south of Santa Rosa Island, along the western side of San Nicholas and Santa Cruz Basins, ringing the southern islands, and hugging the coast (Figure 9). The largest continuous areas of high probability occurred north of San Miguel Island and on the southwest side of Santa Cruz Basin (Figure 9).

High levels of uncertainty in these predictions exists for all three taxa throughout the SCB (Figures 7, 8, & 9). Large areas of uncertainty exist especially for *P. longispina* predictions (Figure 8) as well as Porifera sp., particularly in the northern section of CINMS (Figure 9). *A. dendrochristos* had better certainty in model predictions (Figure 7), although stretches of high uncertainty exists in the western part of the northern portion of CINMS and around San Nicholas Island.

Suitable Habitat Within National Marine Sanctuary Waters

Maxent models predicted small areas of high suitability within CINMS for all taxa, generally southwest of San Miguel Island, southeast of Santa Cruz Island, and around Santa Barbara Island (Figures A2, A3, and A4). While the total percentage of the CINMS area that is suitable habitat for the three DSCS is low (<3% for all taxa, Table 8), the percent of total suitable habitat of the SCB study area that falls in the CINMS is much higher (9-35%, Table 8). Specifically, 35.3% and 27.9% of suitable *A. dendrochristos* SCV habitat (at the 0.75 and 0.5 thresholds, respectively) occurs in the CINMS (Table 8). A smaller percentage of suitable habitat for *P. longispina*, exists in CINMS (15.8% and 9.1% at the 0.75 and 0.5 thresholds, respectively; Table 8). Nearly equal amounts of suitable habitat exists for Porifera sp. in CINM: 15.7% at the 0.5 threshold and 14.9% at the 0.75 threshold (Table 8). CINMS Suitable Habitat is the area of the CINMS predicted to be suitable habitat (at the stated threshold) divided by the total CINMS area between 50-500 m depth (2679 km^2), expressed as a percentage. SCB Suitable Habitat is calculated in the same fashion, the total study area between 50-500 m in SCB is 15,437 km^2. DSCS Habitat Protected by CINMS is the proportion of total SCB suitable habitat area that is located within the CINMS, expressed as a percentage. For example, *A. dendrochristos* had 183.1 km^2 of suitable habitat available at the 0.5 habitat suitability threshold available in the SCB, of which 51.1 km^2 fell within CINMS waters, or 27.9%.

Table 8. Proportion of total Channel Islands National Marine Sanctuary (CINMS) and the Southern California Bight (SCB) that are predicted to be suitable habitat for three DSCS taxa, based on GAM and Maxent models. GAM results were subsetted to only include areas of high certainty (with a CrI range <0.25), and the same process was repeated and reported here as GAM*.

Taxa	Model	Logistic Threshold	CINMS Suitable Habitat	SCB Suitable Habitat	Habitat Protected by CINMS
A. dendrochristos	Maxent	0.5	1.9%	1.2%	27.9%
A. dendrochristos	Maxent	0.75	0.15%	0.11%	35.3%
A. dendrochristos	GAM	0.5	23.0%	26.5%	15.0%
A. dendrochristos	GAM	0.75	15.3%	18.6%	14.3%
A. dendrochristos	GAM*	0.5	9.1%	11.2%	14.1%
A. dendrochristos	GAM*	0.75	9.1%	11.2%	14.1%
P. longispina	Maxent	0.5	0.90%	2.5%	9.1%
P. longispina	Maxent	0.75	0.28%	0.44%	15.8%
P. longispina	GAM	0.5	42.8%	48.1%	15.4%
P. longispina	GAM	0.75	33.2%	35.1%	16.4%
P. longispina	GAM*	0.5	17.1%	15.3%	19.3%
P. longispina	GAM*	0.75	29.3%	44.5%	16.5%
Porifera sp.	Maxent	0.5	2.9%	4.5%	15.7%
Porifera sp.	Maxent	0.75	0.52%	0.89%	14.9%
Porifera sp.	GAM	0.5	31.1%	22.4%	24.0%
Porifera sp.	GAM	0.75	12.1%	11.7%	18.0%
Porifera sp.	GAM*	0.5	2.4%	3.9%	10.8%
Porifera sp.	GAM*	0.75	2.4%	3.8%	10.7%

Relative to the Maxent models, the GAMs generally predicted larger areas of high probability of occurrence within CINMS for all three taxa; however when areas with high uncertainty were accounted for the distributions were much smaller (Figures 7, 8, & 9). GAMs generally predicted areas of high probability on the northern side of both sections of CINMS (Figures A5, A6, and A7). The low uncertainty GAM and Maxent models estimated that the total percentage of CINMS suitable habitat was higher for *P. longispina,* and lower for Porifera sp. and *A. dendrochristos.* About 11-19% of CINMS area has a high probability of occurrence for the three taxa, although the total percentage of high probability areas in the SCB that falls within CINMS is more consistent between the two models for *P. longispina* and Porifera sp. (Table 8).

DISCUSSION

Summary of project goals and results

Predictive models for *A. dendrochristos,* and two DSCS associated with YOY rockfish (*P. longispina* and Porifera sp.) were used to create distribution maps in the SCB. Both presence-absence (GAMs) and presence-only models (Maxent) predicted known presences well (Tables 5 & 7); however important variables for making these predictions varied between modeling methods (Tables 4 & 7). The GAMs, which were developed using the best practices for DSCS species distribution modeling (Winship et al. 2020), found that depth and bottom current direction and velocity were important in predicting the presence for all taxa. Both Maxent and GAMs pointed to several areas outside of CINMS that may be candidates for exploration and potentially additional conservation. Hidden Reef, Santa Catalina, and San Clemente are all areas outside of CINMS that may be important habitat for these three DSCS, as well as their associated fish and invertebrate species.

Model Comparison

Models that include true absence data, such as GAMs, are the preferred modeling method for DSCS SDMs as they provide additional information on conditions that are not suitable for species (Elith et al., 2011; Winship et al., 2020). In this study, model AUC

scores were similar between Maxent and GAMs, implying they both performed well when predicting known presences (and absences for GAMs). These results are similar to the results found in a comparison of several SDMs including Maxent and GAMs (Duque-Lazo et al., 2016); however in the Duque-Lazo et al. (2016) study they found GAM performed better when the model was used in a new study location (i.e. GAMs were more "transferable"). Results from Maxent reflect environmental conditions at occurrence points across the landscape. Thus, results can provide information on what feature a species may be "selecting" for in a landscape, with caveats including sampling bias in the species observations, such as high occurrences in areas that are easier to access for surveying (Elith et al. 2011).

GAM models in this study accounted for spatial autocorrelation, and therefore likely make better inferences than models that do not account for this spatial dependency (Legendre, 1993), such as the Maxent models (Václavík et al., 2012). In addition to the use of presence and absence data, this aspect of accounting for spatial autocorrelation in the GAMs is also considered a best practice for building DSCS SDMs (Winship et al., 2020). These spatial models provide more reliable results as they account for patterns that may be created by unexplained variation in the models.

Measures of uncertainty are important for interpreting model predictions, and areas of low uncertainty and high probability are provided for all GAMs (Figures 7, 8, and 9). These areas of high confidencewere generally distributed throughout the SCB for all three taxa. Areas of agreement between the three taxa include areas north of Santa

Barbara Island, on the banks south of San Nicholas Island, around Santa Catalina and San

Clemente, and in patches west of San Miguel (Figures 7, 8, and 9). While measures of

uncertainty in model predictions were not estimated for Maxent, I recommend future

studies include these via analysis such as trend surface analysis (Václavík et al., 2012).

Environmental Predictors

Interpretation of relationships between probability of taxa occurrences and

environmental predictors should be done with caution. Positional errors in species

occurrences are difficult to detect but can create substantial changes to model results

(Osborne and Leitão, 2009) and mismatches in the scale of predictors can miss important

relationships with the organism of study (Dolan et al., 2008; Rengstorf et al., 2013).

Additionally, as is the case with this study, different models can come to different results

in terms of which variables are important and what the relationship is between the

response and the predictors due to differences in modeling approaches and in the data

used to build the models. With these concepts taken into consideration, information

provided by visual plots (e.g. response plots) and cross-validation (i.e. how often a

variable is selected as an important variable in a model) can provide insight to ecological

processes otherwise difficult to obtain and influence future areas of study (Huff et al.,

2013; Rengstorf et al., 2013; Gugliotti et al., 2019).

Depth was an important variable in all models and is a common, important

variable in SDMs (Bryan and Metaxas, 2007; Davies and Guinotte, 2011; Huff et al.,

2013, Ross & Howell 2013). While DSCS have niches associated with depth (Cairns, 2007), depth can act as a proxy for other correlated environmental variables not included in the models, such as temperature and dissolved oxygen (Garcia et al., 2014). However, in this study I did not find depth correlated with these or other measured covariates. This may be due to the scale at which DO and temperature were estimated by ROMS/NEMURO, which is 100 times greater than the depth measure estimates provided by the California Relief Model. This mismatch in scale may be why depth came out as an important variable in all models, as depth was measured at a finer scale (30 m) and may be a proxy for other variables at a finer scale. The food variables predicted using the ROMS/NEMURO (calculated at a scale of 3 km) may have been too coarse, particularly compared to the scale of depth measurements. This finer resolution may better represent the conditions that DSCS exist in. Additionally, depth may be representing more complex associations between multiple variables. Megafauna biomass and abundance are known to decrease with depth most likely due to loss of available energy (Rex et al., 2006), and competition among DSCS for resources could play a role in distributions (Iken et al., 2001) although competition in the deep sea may not be as large of a driver as it is in shallower rocky reefs (Rex et al., 2006).

The remaining bathymetric variables play a less important role in both maxent and GAM models. FBPI and slope were low contributing variables in all maxent models, and although they came out as important in GAMs (Table 7), there was not a strong relationship between probability and these variables (Figure 6). This agreement between

modeling approaches suggests that these two variables are not good predictors of the three DSCS taxa, which may be due to the scale at which FBPI and slope were calculated (250 m^2 and 90 m^2, respectively). Other BPI scales have been good predictors for DSCS along the California coast (DeVogelaere et al., 2005), and future studies could explore the spatial scales that may be important to DSCS in the SCB.

Northern and eastern current velocities were important covariates in all GAMs, as observed for DSCS in other SDMs (Davies et al., 2008; Huff et al., 2013), likely due to their role in food delivery, larval dispersal, and sediment cleaning (Roberts et al., 2006, Freiwald & Roberts, 2005). GAM response plots showed strong trends between probability of occurrence and current direction/velocity with greater probability in strong northward currents but not in strong southward currents, indicating direction plays an important role (Figure 6). This may be due to large scale processes in the SCB. Currents in the SCB are strongly affected by the California Current, which bends toward the coast of San Diego and then travels north along the coast, through the southern basins, and into the Santa Barbara Channel (Bray et al. 1999, Hickey, 1992, Aaud et al., 2010; Figure A8). An increase in northern current velocity may be connected to increased productivity in the SCB, or increased advection of food present locally (Chavez et al., 1991; Mantyla et al., 2008; Kim et al., 2009).

Eastern currents were also important in all GAMs (Tables 4 & 5). Probability of *A. dendrochristos* was relatively high for weak eastern and western currents, with some negative trends at the highest velocities, although the uncertainty was high for most

western currents (Figure 6). Probability of *P. longispina* was highest at relatively weak western current velocities and Porifera sp. probability was also highest in areas with western velocity currents (Figure 6). These trends may be due to general trends in the environment surveyed, as the data contained a wider range of western current velocities than eastern. There are also certain areas where western current flow is accelerated, particularly out of the western side of the Santa Cruz Basin and into the Santa Barbara Channel east of Santa Cruz Island (Figures A9 & A10), and thus the trend in total magnitude of the current (northern and eastern combined) could be driving this relationship.

Final predictions of the three taxa show some trends in current direction and magnitude, especially in *A. dendrochristos* and *P. longispina* (Figures A9 & A10). High areas of probability occur east of Santa Cruz Island (north of the Footprint), and on the northern side of the banks off San Nicholas Island where a saddle exists between these banks and the banks south of Santa Rosa Island. Both of these areas have a higher probability of occurrence (Figure A9, A10, & A11) which may be connected to increased delivery of food. Considering a cumulative current direction and magnitude may better capture the relationship between DSCS and currents in future models, such as those done for other DSCS species in Ireland (Rengstorf et al., 2013), and Alaska (Rooper et al., 2017).

Huff et al. (2013) created a predictive model for *A. dendrochristos* utilizing the same data set and found the highest abundances in low velocity northern currents, which

differs from this study's results, however predictive maps show general spatial agreement across the SCB. Differences in these results could be due to the types of models used (Huff et al., 2013 utilized a non-spatial GAM to predict counts of *A. dendrochristos*) as well as variables included in the model. Huff et al. (2013) included average January currents as January had the warmest temperatures, which they hypothesized may be related to spawning. I found that seasonal currents were strongly correlated to the average current, (for example average and January currents were correlated at the 0.9 level) and thus used the average. Huff et al. (2013) also had a restricted set of variables in the models that did not include eastern currents or BBPI, which came out as important variables in this study (Tables 4 & 6).

While food was hypothesized to play an important role in DSCS distributions, diatom concentration was not an important variable in the GAMs. Food supplies (detritus, diatom, phytoplankton and zooplankton) were highly collinear with certain environmental variables (temperature and dissolved oxygen), which are also important to DSCS metabolic processes (Roberts, 2009, Gugliottie et al., 2019). It is possible that the spatial or temporal scales used for diatom concentration (and its correlated variables including temperature and dissolved oxygen) were too broad to effectively capture a relationship with the taxa in the GAM models. Food supply, temperature, and dissolved oxygen estimates were originally calculated at ~3 km resolution and averaged over many years. Other, finer-scale variables, such as depth which was calculated at a 30 m resolution, may better capture the conditions DSCS are experiencing.

Scale plays a critical role in predictions for SDMs as DSCS are sessile organisms that require suitable conditions at their location, thus scales that are too large may mismatch localized conditions (Dolan et al., 2008). In this study, bathymetry data (depth, slope, BBPI, and FBPI) used was at a 30 m resolution, while all other variables, such as currents and temperature, were estimated at the 3 km scale and were interpolated down to match the 30 m resolution for modeling. The broad scale variables are likely insufficiently describing the localized environments where patches of DSCS (or solitary DSCS) can occur (Tissot et al., 2006), which in turn are likely adding to error in the models (Rengstorf et al., 2013). These broad scale variables may be better proxies of landscape-wide patterns; for example, currents may be acting as a broad scale proxy for food in the region (Hyrenbach and Veit, 2003, Roemmich & McGowan, 1995). Ocean circulation patterns in the SCB and resulting nutrient and food availability can fluctuate from a daily to a decadal scale. The Southern California Bight is a very complex system where the entire system can be flushed within a matter of days (Hickey 1992). During El Niño years, ocean circulation in the region is generally strengthened and currents broaden in the poleward inshore countercurrent (Dever and Winant, 2002). During La Niña years, these patterns weaken, and strong winds result in greater off-shore flow and sustained upwelling (Dever & Winant 2002, Lynn & Bograd 2002). While DSCS are long-lived and thus large-scale patterns in climate and food availability may be important, an additional metric that captures what areas provide consistent food to DSCS on a daily basis might improve models. Additionally, a measure of food delivery to the bottom on a

smaller spatial scale may better capture the relationship between DSCS and food availability.

Suitable Habitat Within National Marine Sanctuary Waters

Most taxa had less than 20% suitable habitat in the CINMS (Table 8). *A. dendrochristos* was an exception, as it had a relatively high percentage of habitat in CINMS based on Maxent predictions (Table 8). CINMS covers about 25% of the SCB study area (waters within the SCB between 50-500 m), which provides a metric for comparing the amount of suitable DSCS habitat inside and outside CINMS. If the amount of total SCB habitat protected by CINMS (Table 8) is around this value of 25%, that suggests that the CINMS is protecting DSCS habitat at a scale proportional to its size; however, most predictions fell below this threshold suggesting a higher proportion of DSCS exists outside CINMS. The majority of suitable habitat areas inside the CINMS occurred at Piggy Bank and the Footprint southeast of Santa Cruz Island. These areas are known hot spots identified by previous SDMs (Huff et al., 2013; Salgado et al., 2018) and are currently protected as Essential Fish Habitat. Hot spots for Porifera sp. based on GAMs were scattered throughout the CINMS (Figure A7), which is consistent with the widespread and abundant distribution of the taxa throughout the Bight. Both *P. longispina* and Porifera sp. had high probability of occurrence areas on the northern edge of CINMS, which may be connected to higher productivity and nutrient cycling in the Santa Barbara Channel (Bray et al. 1999, Hickey 1992). High probability areas for *A.*

dendrochristos and *P. longispina* exist west of San Miguel Island. This area had fewer surveys than other regions of CINMS, and were generally surveyed less due to intense wind exposure on the west side of the Channel Islands (A. Lauermann, pers. Comm., 2020). Any opportunities to explore this region as well as other areas for conservation consideration outside the CINMS should be taken.

Threshold analyses used in this study come with caveats, specifically that the 0.5 and 0.75 cutoffs are somewhat arbitrary and may not have a direct ecological interpretation (Osborne et al., 2001). It can be easy to assume an output, for either Maxent or GAMs, greater than 0.5 would be associated with presences, and those less than with absences, but it is entirely possible for an area that is predicted to be highly probable is in fact unsuitable (Osborne et al., 2001). Future analyses could consider less subjective thresholds, such as ones that optimize sensitivity and specificity (Liu et al., 2005).

Management Implications and Future Research

While the extensive data collected over the last few decades have provided the baseline for this and many other studies, human impacts and climate change has and will continue to pose a threat to DSCS (Roemmich and McGowan, 1995; Lunden et al., 2014; Gómez et al., 2018). Current and future threats still exist in the form of changing environments. For example, from 2005 to 2014, a large die off in gorgonian deep-sea corals was observed around Anacapa (Etnoyer et al., 2015), followed by die offs along

the central California coast in the fall of 2016 (California Department of Fish and

Wildlife, Marine Region, 2017). Laboratory experiments have revealed these die offs are

likely due to climate change, specifically prolonged exposure to high temperatures

(Gugliottie et al., 2019). While my study did not focus on the species that were

documented in these events, this highlights the potential for species distributions to have

changed from the time of data collection due to acute or chronic impacts of stressors such

as environmentally driven die-offs.

Historically one of the largest threats to DSCS in the SCB is bottom trawl fishing,

which has recently been banned throughout the majority of deep waters in the SCB

(NMFS, 2019). The ban represents a significant development in the protections for

DSCS, but fishing still poses a threat to DSCS species via lost gear pollution, which can

have direct impacts to DSCS (Watters et al., 2010) and can abort dive missions via ROV

entanglement (A. Lauermann, pers. Comm., 2020). Finding a balance between

conservation and commercial fisheries has been an ongoing challenge in the SCB over

the last few decades, and will continue to be in the future (Love et al., 1998; Yoklavich et

al., 2018). Continued advances in predictive modeling can help direct future surveys in

the SCB that can help with future decision-making processes.

Although the cost of deep-sea surveying is high, it is critical to continue gathering

data on DSCS and their environments to understand their current distributions and the

state of their habitats. Current models made for DSCS may reflect realized niches that

have been constrained due to extensive historical bottom trawling along the west coast of

North America (Yoklavich et al., 2018). Assuming current distributions may be dictated by historic bottom trawling throughout the SCB, future distributions of DSCS may change due to the new closures. Future distributions of DSCS will also reflect newer threats to DSCS such as climate change. For example, currents were an important predictor of DSCS in this study, however trends in the strength and temperature of these currents has been shifting and will continue to shift over the coming decades (Doney et al., 2009). Additional data collection on ocean conditions moving forward could allow for updating these models and potentially making predictions for where DSCS may exist in the future.

All models include some level of uncertainty, and the predictions made for the three taxa included areas of high uncertainty. Unfortunately, large areas in CINMS had high uncertainty, particularly for Porifera sp., but many areas exist outside of CINMS that are predicted to have a high probability of occurrence with relatively low uncertainty (Figures 7, 8, & 9). Specifically, areas near Hidden Reef had high probability and low uncertainty for *A. dendrochristos* and *P. longispinga* (Figures 7 & 8). Additionally, all three taxa had areas of high probability and low uncertainty on the banks south of San Nicholas Island, in additions to areas around San Clemente and Santa Catalina Island (Figures 7, 8, & 9). This suggests that these areas may indeed be a 'hot spot' for DSCS, since these locations have also appeared as an area of interest in SDMs for other taxa (Guinotte and Davies, 2014; Salgado et al., 2018, Huff et al., 2013). Areas around San Clemente and Santa Catalina Islands were designated as "highest priority

recommendations for conservation-focused research" due to a high probability of DSCS occurrence and bottom-contact fishing in the area (Salgado et al., 2018). Hidden Reef was also found to be an area for high *A. dendrochristos* frequency (Huff et al., 2013), which emphasizes the potential importance of this area to DSCS and their associated species.

The high cost of surveying deep-sea habitats hinders our ability to study DSCS, but SDMs such as those provided in this study can help to focus future survey and conservation efforts. Predicted hot spots identified here are consistent with other studies (Huff et al., 2013, Etnoyer et al., 2018), and are also expected to be of benefit to commercially important rockfish species given their associations with Porifera sp. and *P. longispina* (Henderson et al., 2020). Threats to DSCS and their associated species will persist into the future, and strategic management and advances in our understanding of their ecology will be critical in creating a sustainable ecosystem in the SCB.

REFERENCES

Auster, P. (2005). Are deep-water corals important habitats for fishes?. In: Freiwald A., Roberts J.M. (eds) Cold-Water Corals and Ecosystems. Erlangen Earth Conference Series. Springer, Berlin, Heidelberg. doi:10.1007/3-540-27673-4_39.

Baillon, S., Hamel, J.-F., Wareham, V. E., and Mercier, A. (2012). Deep cold-water corals as nurseries for fish larvae. Frontiers in Ecology and the Environment 10, 351–356. doi:10.1890/120022.

Bazzichetto, M., Malavasi, M., Bartak, V., Acosta, A. T. R., Rocchini, D., and Carranza, M. L. (2018). Plant invasion risk: A quest for invasive species distribution modelling in managing protected areas. Ecological Indicators 95, 311–319. doi:10.1016/j.ecolind.2018.07.046.

Boch, C. A., DeVogelaere, A., Burton, E., King, C., Lord, J., Lovera, C., et al. (2019). Coral Translocation as a Method to Restore Impacted Deep-Sea Coral Communities. Front. Mar. Sci. 6. doi:10.3389/fmars.2019.00540.

Boland, R. C., and Parrish, F. A. (2005). A description of fish assemblages in the black coral beds off Lahaina, Maui, Hawai 'i. Pacific Science 59, 411–420.

Broquet, G., Edwards, C. A., Moore, A. M., Powell, B. S., Veneziani, M., and Doyle, J. D. (2009). Application of 4D-Variational data assimilation to the California Current System. Dynamics of Atmospheres and Oceans 48, 69–92. doi:10.1016/j.dynatmoce.2009.03.001.

Bryan, T. L., and Metaxas, A. (2007). Predicting suitable habitat for deep-water gorgonian corals on the Atlantic and Pacific Continental Margins of North America. Marine Ecology Progress Series 330, 113–126.

Caldow, C., Clarke, M. E., Coleman, H. M., Duncan, E., Everett, M. V., Hourigan, T. F., et al. (2019). West Coast Deep-Sea Coral Initiative Science Plan (2018-2021).

Chavez, F. P., Barber, R. T., Kosro, P. M., Huyer, A., Ramp, S. R., Stanton, T. P., et al. (1991). Horizontal transport and the distribution of nutrients in the Coastal Transition Zone off northern California: Effects on primary production, phytoplankton biomass and species composition. Journal of Geophysical Research: Oceans 96, 14833–14848. doi:https://doi.org/10.1029/91JC01163.

CINMS (2012). Channel Islands National Marine Sanctuary Science Needs Assessment: Habitat Characterization. Available at: (http://sanctuaries.noaa.gov/science/assessment/pdfs/cinms_habitat_characterizati on.pdf).

Clark, M. R., Tittensor, D., Brewin, P., Schlacher, T., Rowden, A., and Stocks, K. (2006). Seamounts, deep-sea corals and fisheries: vulnerability of deep-sea corals to fishing on seamounts beyond areas of national jurisdiction. Cambridge, U.K.: UNEP WCMC.

Dailey, M. D., Reish, D. J., and Anderson, J. W. eds. (1994). Ecology of the Southern California Bight: A Synthesis and Interpretation. First Printing edition. Berkeley: University of California Press.

Davies, A. J., Duineveld, Gerard C. A., Lavaleye, Marc S. S., Bergman, Magda J. N., van Haren, H., and Roberts, J. M. (2009). Downwelling and deep-water bottom currents as food supply mechanisms to the cold-water coral Lophelia pertusa (Scleractinia) at the Mingulay Reef Complex. Limnol. Oceanogr. 54, 620–629. doi:10.4319/lo.2009.54.2.0620.

Davies, A. J., and Guinotte, J. M. (2011). Global Habitat Suitability for Framework-Forming Cold-Water Corals. PLOS ONE 6, e18483. doi:10.1371/journal.pone.0018483.

Davies, A. J., Wisshak, M., Orr, J. C., and Murray Roberts, J. (2008). Predicting suitable habitat for the cold-water coral Lophelia pertusa (Scleractinia). Deep Sea Research Part I: Oceanographic Research Papers 55, 1048–1062. doi:10.1016/j.dsr.2008.04.010.

Dayton, P. K., Tegner, M. J., Edwards, P. B., and Riser, K. L. (1998). Sliding Baselines, Ghosts, and Reduced Expectations in Kelp Forest Communities. Ecological Applications 8, 309–322. doi:10.1890/1051-0761(1998)008[0309:SBGARE]2.0.CO;2.

de Froe, E., Rovelli, L., Glud, R. N., Maier, S. R., Duineveld, G., Mienis, F., et al. (2019). Benthic Oxygen and Nitrogen Exchange on a Cold-Water Coral Reef in the North-East Atlantic Ocean. Front. Mar. Sci. 6. doi:10.3389/fmars.2019.00665.

DeVogelaere, A. P., Burton, E. J., Trejo, T., King, C. E., Clague, D. A., Tamburri, M. N., et al. (2005). "Deep-sea corals and resource protection at the Davidson Seamount, California, U.S.A.," in Cold-Water Corals and Ecosystems Erlangen Earth

Conference Series., eds. A. Freiwald and J. M. Roberts (Berlin/Heidelberg: Springer-Verlag), 1189–1198. doi:10.1007/3-540-27673-4_61.

Dodds, L. A., Roberts, J. M., Taylor, A. C., and Marubini, F. (2007). Metabolic tolerance of the cold-water coral Lophelia pertusa (Scleractinia) to temperature and dissolved oxygen change. Journal of Experimental Marine Biology and Ecology 349, 205–214. doi:10.1016/j.jembe.2007.05.013.

Dolan, M. F. J., Grehan, A. J., Guinan, J. C., and Brown, C. (2008). Modelling the local distribution of cold-water corals in relation to bathymetric variables: Adding spatial context to deep-sea video data. Deep Sea Research Part I: Oceanographic Research Papers 55, 1564–1579. doi:10.1016/j.dsr.2008.06.010.

Drexler, M., and Ainsworth, C. H. (2013). Generalized Additive Models Used to Predict Species Abundance in the Gulf of Mexico: An Ecosystem Modeling Tool. PLOS ONE 8, e64458. doi:10.1371/journal.pone.0064458.

Duineveld, G., Lavaleye, M., and Berghuis, E. (2004). Particle flux and food supply to a seamount cold-water coral community (Galicia Bank, NW Spain). Marine Ecology Progress Series 277, 13–23. doi:10.3354/meps277013.

Duque-Lazo, J., van Gils, H., Groen, T. A., and Navarro-Cerrillo, R. M. (2016). Transferability of species distribution models: The case of Phytophthora cinnamomi in Southwest Spain and Southwest Australia. Ecological Modelling 320, 62–70. doi:10.1016/j.ecolmodel.2015.09.019.

Eakins, B. (2003). U.S. Coastal relief model — Central Pacific. Available at: www.ngdc.noaa.gov/mgg/coastal/ grddas07/grddas07.htm (accessed 15 April 2012).

Edwards, C. A., Moore, A. M., Hoteit, I., and Cornuelle, B. D. (2015). Regional Ocean Data Assimilation. Annual Review of Marine Science 7, 21–42. doi:10.1146/annurev-marine-010814-015821.

Elith, J., Phillips, S. J., Hastie, T., Dudík, M., Chee, Y. E., and Yates, C. J. (2011). A statistical explanation of MaxEnt for ecologists. Diversity and Distributions 17, 43–57. doi:10.1111/j.1472-4642.2010.00725.x.

Erisman, B. E., Allen, L. G., Claisse, J. T., Pondella, D. J., Miller, E. F., and Murray, J. H. (2011). The illusion of plenty: hyperstability masks collapses in two recreational fisheries that target fish spawning aggregations. Can. J. Fish. Aquat. Sci. 68, 1705–1716. doi:10.1139/f2011-090.

Etnoyer, P. J., Wagner, D., Fowle, H. A., Poti, M., Kinlan, B., Georgian, S. E., et al. (2017). Models of habitat suitability, size, and age-class structure for the deep-sea black coral Leiopathes glaberrima in the Gulf of Mexico. Deep Sea Research Part II: Topical Studies in Oceanography. doi:10.1016/j.dsr2.2017.10.008.

Etnoyer, P., and Warrenchuk, J. (2007). A catshark nursery in a deep gorgonian field in the Mississippi Canyon, Gulf of Mexico.

Fiechter, J., Huff, D. D., Martin, B. T., Jackson, D. W., Edwards, C. A., Rose, K. A., et al. (2015). Environmental conditions impacting juvenile Chinook salmon growth off central California: An ecosystem model analysis. Geophysical Research Letters 42, 2910–2917. doi:10.1002/2015GL063046.

Fielding, A. H., and Bell, J. F. (1997). A review of methods for the assessment of prediction errors in conservation presence/absence models. Environmental Conservations 24, 38–49.

Fossa, J. H., Mortensen, P. B., and Furevik, D. M. (2002). The deep-water coral Lophelia pertusa in Norwegian waters: distribution and fishery impacts. Hydrobiologia 471, 1–12.

Freiwald, A. (2002). Reef-forming cold-water corals G. Wefer, D. Billett, D. Hebbeln, B.B. Jorgensen, M. Schluter, T. Van Weering (Eds.) pp. 365-385. Springer-Verlag.

Freiwald, A., and Roberts, J. M. eds. (2005). Cold-water corals and ecosystems. Berlin: Springer.

Gage, J. D., Roberts, J. M., Hartley, J. P., and Humphery, J. D. (2005). Potential impacts of deep-sea trawling on the benthic ecosystem along the Northern European continental margin: a review. in Benthic Habitats and the Effects of Fishing (American Fisheries Society), 503–517. Available at: https://researchportal.hw.ac.uk/en/publications/potential-impacts-of-deep-sea-trawling-on-the-benthic-ecosystem-a [Accessed December 11, 2020].

Garcia, H. E., Lacarnini, R. A., Boyer, T. P., Antonov, J. I., Mishonov, A. V., Baranova, O. K., et al. (2014). "World Ocean Atlas 2013," in Volume 3: Dissolved Oxygen, Apparent Oxygen Utilization, and Oxygen Saturation, eds. S. Levitus and A. Mishonov (Silver Spring, MD: NOAA Atlas NESDIS 75).

Gelfand, A. E., Silander, J. A., Wu, S. S., Latimer, A., Lewis, P. O., Rebelo, A. G., et al. (2006). Explaining species distribution patterns through hierarchical modeling. Bayesian Analysis 1, 41–91.

Gómez, C. E., Wickes, L., Deegan, D., Etnoyer, P. J., and Cordes, E. E. (2018). Growth and feeding of deep-sea coral Lophelia pertusa from the California margin under simulated ocean acidification conditions. PeerJ 6, e5671. doi:10.7717/peerj.5671.

Grüss, A., Drexler, M., and Ainsworth, C. H. (2014). Using delta generalized additive models to produce distribution maps for spatially explicit ecosystem models. Fisheries Research 159, 11–24. doi:10.1016/j.fishres.2014.05.005.

Gugliotti, E. F., DeLorenzo, M. E., and Etnoyer, P. J. (2019). Depth-dependent temperature variability in the Southern California bight with implications for the cold-water gorgonian octocoral Adelogorgia phyllosclera. Journal of Experimental Marine Biology and Ecology 514–515, 118–126. doi:10.1016/j.jembe.2019.03.010.

Guinotte, J. M., and Davies, A. J. (2014). Predicted Deep-Sea Coral Habitat Suitability for the U.S. West Coast. PLOS ONE 9, e93918. doi:10.1371/journal.pone.0093918.

Heifetz, J., Stone, R., and Shotwell, S. (2009). Damage and disturbance to coral and sponge habitat of the Aleutian Archipelago. Marine Ecology Progress Series 397, 295–303. doi:10.3354/meps08304.

Held, L., Schrödle, B., and Rue, H. (2010). "Posterior and Cross-validatory Predictive Checks: A Comparison of MCMC and INLA," in Statistical Modelling and Regression Structures: Festschrift in Honour of Ludwig Fahrmeir, eds. T. Kneib and G. Tutz (Heidelberg: Physica-Verlag HD), 91–110. doi:10.1007/978-3-7908-2413-1_6.

Henderson, M., Huff, D., and Yoklavich, M. (2020). Deep-Sea Coral and Sponge Taxa Increase Demersal Fish Diversity and the Probability of Fish Presence. Frontiers in Marine Science 7, 1–19. doi:10.3389/fmars.2020.593844.

Henrich, R., Freiwald, A., and Shipboard Party (1997). The Lophelia reef on Sula ridge, mid-Norweigian shelf.

Hickey, B. M. (1992). Circulation over the Santa Monica-San Pedro Basin and Shelf. Progress in Oceanography 30, 37–115. doi:10.1016/0079-6611(92)90009-O.

Hickey, B. M., Dobbins, E. L., and Allen, S. E. (2003). Local and remote forcing of currents and temperature in the central Southern California Bight. J. Geophys. Res. 108, 3081. doi:10.1029/2000JC000313.

Hijmans, R. J., Phillips, S., Leathwich, J., and Elith, J. (2017). dismo: Species Distribution Modeling. Available at: https://CRAN.R-project.org/package=dismo.

Hourigan, T. F., Etnoyer, P. J., and Cairns, S. D. (2017). The State of Deep-Sea Coral and Sponge Ecosystems of the United States. Silver Spring, MD.

Huff, D., Yoklavich, M., Love, M., Watters, D., Chai, F., and Lindley, S. (2013). Environmental factors that influence the distribution, size, and biotic relationships of the Christmas tree coral Antipathes dendrochristos in the Southern California Bight. Marine Ecology Progress Series 494, 159–177. doi:10.3354/meps10591.

Kariyawasam, C., Kadupitiya, H., Ratnayake, R., Hettiarchchi, A., and Ratnayake, R. (2017). Identification of High-Risk Agro-Ecological Regions using Species Distribution Modeling of Priority Invasive Species in Sri Lanka. Ind. Jour. Plant Gene. Resour. 30, 228. doi:10.5958/0976-1926.2017.00028.6.

Kim, H.-J., Miller, A. J., McGowan, J., and Carter, M. L. (2009). Coastal phytoplankton blooms in the Southern California Bight. Progress in Oceanography 82, 137–147. doi:10.1016/j.pocean.2009.05.002.

Kiriakoulakis, K., Fisher, E., Wolff, G. A., Freiwald, A., Grehan, A., and Roberts, J. M. (2005). "Lipids and nitrogen isotopes of two deep-water corals from the North-East Atlantic: initial results and implications for their nutrition," in Cold-water corals and ecosystems (Springer), 715–729.

Kishi, M. J., Ito, S., Megrey, B. A., Rose, K. A., and Werner, F. E. (2011). A review of the NEMURO and NEMURO.FISH models and their application to marine ecosystem investigations. Journal of Oceanography; Tokyo 67, 3–16. doi:http://dx.doi.org/10.1007/s10872-011-0009-4.

Kishi, M. J., Kaeriyama, M., Ueno, H., and Kamezawa, Y. (2010). The effect of climate change on the growth of Japanese chum salmon (Oncorhynchus keta) using a bioenergetics model coupled with a three-dimensional lower trophic ecosystem model (NEMURO). Deep Sea Research Part II: Topical Studies in Oceanography 57, 1257–1265. doi:10.1016/j.dsr2.2009.12.013.

Kishi, M. J., Nakajimia, K., Fujii, M., and Hashioka, T. (2009). Environmental factors which affect growth of Japanese common squid, Todarodes pacificus, analyzed by

a bioenergetics model coupled with a lower trophic ecosystem model. Journal of Marine Systems 78, 278–287.

Lessard-Pilon, S. A., Podowski, E. L., Cordes, E. E., and Fisher, C. R. (2010). Megafauna community composition associated with Lophelia pertusa colonies in the Gulf of Mexico. Deep Sea Research Part II: Topical Studies in Oceanography 57, 1882–1890. doi:10.1016/j.dsr2.2010.05.013.

Lindgren, F., and Rue, H. (2015). Bayesian spatial modelling with R-INLA.

Liu, C., Berry, P. M., Dawson, T. P., and Pearson, R. G. (2005). Selecting thresholds of occurrence in the prediction of species distributions. Ecography 28, 385–393. doi:https://doi.org/10.1111/j.0906-7590.2005.03957.x.

Love, M., Caselle, J. E., and Van Buskirk, W. (1998). A severe decline in the commercial passenger fishing vessel rockfish (Sebastes spp.) catch in the Southern California Bight, 1980-1996. Available at: http://calcofi.org/publications/calcofireports/v39/Vol_39_Love_etal.pdf [Accessed October 14, 2017].

Love, M. S., and Yoklavich, M. (2008). Habitat characteristics of juvenile cowcod, Sebastes levis (Scorpaenidae), in Southern California. Environmental Biology of Fishes 82, 195–202. doi:10.1007/s10641-007-9290-x.

Love, M. S., Yoklavich, M., and Schroeder, D. M. (2009). Demersal fish assemblages in the Southern California Bight based on visual surveys in deep water. Environmental Biology of Fishes 84, 55–68. doi:10.1007/s10641-008-9389-8.

Lumsden, S., Hourigan, T., Bruckner, A., and Dorr, G. (2007). The State of Deep Coral Ecosystems of the United States. NOAA Technical Memorandum CRCP-3.

Lundblad, E., Wright, D. J., Miller, J., Larkin, E. M., Rinehart, R., Anderson, S. M., et al. (2006). Classifying Benthic Terrains with Multibeam Bathymetry, Bathymetric Position and Rugosity: Tutuila, American Samoa. Marine Geodesy 29, 89–111.

Lunden, J. J., McNicholl, C. G., Sears, C. R., Morrison, C. L., and Cordes, E. E. (2014). Acute survivorship of the deep-sea coral Lophelia pertusa from the Gulf of Mexico under acidification, warming, and deoxygenation. Front. Mar. Sci. 1. doi:10.3389/fmars.2014.00078.

Lynn, R. J., and Simpson, J. J. (1987). The California Current system: The seasonal variability of its physical characteristics. Journal of Geophysical Research: Oceans 92, 12947–12966. doi:10.1029/JC092iC12p12947.

Mantyla, A. W., Bograd, S. J., and Venrick, E. L. (2008). Patterns and controls of chlorophyll-a and primary productivity cycles in the Southern California Bight. Journal of Marine Systems 73, 48–60. doi:10.1016/j.jmarsys.2007.08.001.

Moore, A. M., Arango, H. G., Broquet, G., Powell, B. S., Weaver, A. T., and Zavala-Garay, J. (2011). The Regional Ocean Modeling System (ROMS) 4-dimensional variational data assimilation systems. Progress in Oceanography 91, 34–49. doi:10.1016/j.pocean.2011.05.004.

Mortensen, P. B. (2001). Aquarium observations on the deep-water coral Lophelia pertusa (L., 1758) (Scleractinia) and seleceted associated invertebrates. Ophelia 54, 83–104.

Moser, H. G., Charter, R. L., Watson, W., Ambrose, D. A., Butler, J. L., Charter, S. R., et al. (2000). Abundance and distribution of rockfish (Sebastes) larvae in the Southern California Bight in relation to environmental conditions and fishery exploitation. Calif. Coop. Oceanic Fish. Invest. Rep 41, 132–147.

Nakao, K., Higa, M., Tsuyama, I., Matsui, T., Horikawa, M., and Tanaka, N. (2013). Spatial conservation planning under climate change: Using species distribution modeling to assess priority for adaptive management of Fagus crenata in Japan. Journal for Nature Conservation 21, 406–413. doi:10.1016/j.jnc.2013.06.003.

NMFS (2019). Magnuson-Stevens Act Provisions; Fisheries Off West Coast States; Pacific Coast Groundfish Fishery; Pacific Fishery Management Plan; Amendment 28. National Marine Fisheries Service (NMFS), National Oceanic and Atmospheric Administration (NOAA), Commerce Available at: https://www.federalregister.gov/documents/2019/11/19/2019-24684/magnuson-stevens-act-provisions-fisheries-off-west-coast-states-pacific-coast-groundfish-fishery [Accessed November 23, 2020].

Oberle, F. K. J., Storlazzi, C. D., and Hanebuth, T. J. J. (2016). What a drag: Quantifying the global impact of chronic bottom trawling on continental shelf sediment. Journal of Marine Systems 159, 109–119. doi:10.1016/j.jmarsys.2015.12.007.

Ohashi, H., Kominami, Y., Higa, M., Koide, D., Nakao, K., Tsuyama, I., et al. (2016). Land abandonment and changes in snow cover period accelerate range expansions of sika deer. Ecology and Evolution 6, 7763–7775. doi:10.1002/ece3.2514.

ONMS (2009). Channel Islands National Marine Sanctuary Condition Report 2009. U.S. Department of Commerce, National Oceanic and Atmospheric Administration, Office of National Marine Sanctuaries, Silver Spring, MD. 60pp.

Osborne, P. E., Alonso, J. C., and Bryant, R. G. (2001). Modelling landscape-scale habitat use using GIS and remote sensing: a case study with great bustards. Journal of Applied Ecology 38, 458–471. doi:https://doi.org/10.1046/j.1365-2664.2001.00604.x.

Osborne, P. E., and Leitão, P. J. (2009). Effects of species and habitat positional errors on the performance and interpretation of species distribution models. Diversity and Distributions 15, 671–681. doi:https://doi.org/10.1111/j.1472-4642.2009.00572.x.

Pham, C. K., Diogo, H., Menezes, G., Porteiro, F., Braga-Henriques, A., Vandeperre, F., et al. (2014). Deep-water longline fishing has reduced impact on Vulnerable Marine Ecosystems. Scientific Reports 4, 4837. doi:10.1038/srep04837.

Phillips, S. J., Anderson, R. P., and Schapire, R. E. (2006). Maximum entropy modeling of species geographic distributions. Ecological Modelling, 29.

Pirtle, J. L. (2005). Habitat-based assessment of structure-forming megafaunal invertebrates and fishes on Cordell Bank, California.

R Core Team (2019). R: A language and environment for statistical computing. R Foundation for Statistical Computing, Vienna, Austria. Available at: https://www.R-project.org/.

Rengstorf, A. M., Yesson, C., Brown, C., and Grehan, A. J. (2013). High-resolution habitat suitability modelling can improve conservation of vulnerable marine ecosystems in the deep sea. J. Biogeogr. 40, 1702–1714. doi:10.1111/jbi.12123.

Rex, M. A., Etter, R. J., Morris, J. S., Crouse, J., McClain, C. R., Johnson, N. A., et al. (2006). Global bathymetric patterns of standing stock and body size in the deep-sea benthos. Marine Ecology Progress Series 317, 1–8. doi:10.3354/meps317001.

Roemmich, D., and McGowan, J. (1995). Climatic Warming and the Decline of Zooplankton in the California Current. Science 267, 1324–1326.

Rogers, A. D., Taylor, M. L., Kemp, K., Yesson, C., and Davies, A. J. (2015). The Diseases of Deep-Water Corals (eds C. M. Woodley, C. A. Downs, A. W. Bruckner, J. W. Porter and S. B. Galloway). John Wiley & Sons, Inc, Hoboken, NJ. Available at:

http://onlinelibrary.wiley.com/doi/10.1002/9781118828502.ch32/summary [Accessed February 27, 2018].

Rooper, C. N., Zimmermann, M., and Prescott, M. M. (2017). Comparison of modeling methods to predict the spatial distribution of deep-sea coral and sponge in the Gulf of Alaska. Deep Sea Research Part I: Oceanographic Research Papers 126, 148–161. doi:10.1016/j.dsr.2017.07.002.

Ross, R. E., and Howell, K. L. (2013). Use of predictive habitat modelling to assess the distribution and extent of the current protection of 'listed' deep-sea habitats. Diversity and Distributions 19, 433–445. doi:https://doi.org/10.1111/ddi.12010.

Rue, H., Martino, S., and Chopin, N. (2009). Approximate Bayesian inference for latent Gaussian models by using integrated nested Laplace approximations. Journal of the Royal Statistical Society: Series B (Statistical Methodology) 71, 319–392. doi:10.1111/j.1467-9868.2008.00700.x.

Song, H., Edwards, C. A., Moore, A. M., and Fiechter, J. (2016). Data assimilation in a coupled physical–biogeochemical model of the California Current System using an incremental lognormal 4-dimensional variational approach: Part 1—Model formulation and biological data assimilation twin experiments. Ocean Modelling 106, 131–145. doi:10.1016/j.ocemod.2016.04.001.

Stone, R. P. (2014). NOAA Prof. Paper NMFS 16: The ecology of deep-sea coral and sponge habitats of the central Aleutian Islands of Alaska. National Marine Fisheries Service, NOAA doi:10.7755/PP.16.

Suárez-Seoane, S., Osborne, P. E., and Alonso, J. C. (2002). Large-scale habitat selection by agricultural steppe birds in Spain: identifying species–habitat responses using generalized additive models. Journal of Applied Ecology 39, 755–771. doi:https://doi.org/10.1046/j.1365-2664.2002.00751.x.

Tissot, B. N., Yoklavich, M. M., Love, M. S., York, K., and Amend, M. (2006). Benthic invertebrates that form habitat on deep banks off southern California, with special reference to deep sea coral. Fishery Bulletin 104, 167–181.

Tittensor, D. P., Baco, A. R., Brewin, P. E., Clark, M. R., Consalvey, M., Hall-Spencer, J., et al. (2009). Predicting global habitat suitability for stony corals on seamounts. Journal of Biogeography 36, 1111–1128. doi:10.1111/j.1365-2699.2008.02062.x.

Tong, R., Purser, A., Guinan, J., and Unnithan, V. (2013). Modeling the habitat suitability for deep-water gorgonian corals based on terrain variables. Ecological Informatics 13, 123–132. doi:10.1016/j.ecoinf.2012.07.002.

Václavík, T., Kupfer, J. A., and Meentemeyer, R. K. (2012). Accounting for multi-scale spatial autocorrelation improves performance of invasive species distribution modelling (iSDM). Journal of Biogeography 39, 42–55. doi:https://doi.org/10.1111/j.1365-2699.2011.02589.x.

Veneziani, M., Edwards, C. A., Doyle, J. D., and Foley, D. (2009). A central California coastal ocean modeling study: 1. Forward model and the influence of realistic versus climatological forcing. J. Geophys. Res. 114, C04015. doi:10.1029/2008JC004774.

Wagner, D., Luck, D. G., and Toonen, R. J. (2012). The biology and ecology of black corals (Cnidaria: Anthozoa: Hexacorallia: Antipatharia). Adv. Mar. Biol. 63, 67–132. doi:10.1016/B978-0-12-394282-1.00002-8.

Wang, X. Y., Huang, X. L., Jiang, L. Y., and Qiao, G. X. (2010). Predicting potential distribution of chestnut phylloxerid (Hemiptera: Phylloxeridae) based on GARP and Maxent ecological niche models. Journal of Applied Entomology 134, 45–54. doi:https://doi.org/10.1111/j.1439-0418.2009.01447.x.

Warren, D. L., and Seifert, S. N. (2011). Ecological niche modeling in Maxent: the importance of model complexity and the performance of model selection criteria. Ecol Appl 21, 335–342. doi:10.1890/10-1171.1.

Watters, D. L., Yoklavich, M. M., Love, M. S., and Schroeder, D. M. (2010). Assessing marine debris in deep seafloor habitats off California. Marine Pollution Bulletin 60, 131–138.

Werner, F. E., Ito, S.-I., Megrey, B. A., and Kishi, M. J. (2007). Synthesis of the NEMURO model studies and future directions of marine ecosystem modeling. Ecological Modelling 202, 211–223. doi:10.1016/j.ecolmodel.2006.08.019.

White, M., Mohn, C., Stigter, H. de, and Mottram, G. (2005). "Deep-water coral development as a function of hydrodynamics and surface productivity around the submarine banks of the Rockall Trough, NE Atlantic," in Cold-Water Corals and Ecosystems Erlangen Earth Conference Series. (Springer, Berlin, Heidelberg), 503–514. doi:10.1007/3-540-27673-4_25.

Winship, A. J., Thorson, J. T., Clarke, M. E., Coleman, H. M., Costa, B., Georgian, S. E., et al. (2020). Good Practices for Species Distribution Modeling of Deep-Sea Corals and Sponges for Resource Management: Data Collection, Analysis, Validation, and Communication. Frontiers in Marine Science 7, 303. doi:10.3389/fmars.2020.00303.

Wood, S. (2019). mgcv: Mixed GAM Computation Vehicle with Automatic Smoothness Estimation. Available at: https://cran.r-project.org/web/packages/mgcv/index.html.

Wood, S., Pya, N., and Saefken, B. (2016). Smoothing parameter and model selection for general smooth models. Journal of the American Statistical Association 111, 1548–1575. doi:http://dx.doi.org/10.1080/01621459.2016.1180986.

Yesson, C., Taylor, M. L., Tittensor, D. P., Davies, A. J., Guinotte, J., Baco, A., et al. (2012). Global habitat suitability of cold-water octocorals: Global distribution of deep-sea octocorals. Journal of Biogeography 39, 1278–1292. doi:10.1111/j.1365-2699.2011.02681.x.

Yoklavich, M., and Love, M. (2005). CHRISTMAS TREE CORALS: ANew SPECIES DISCOVERED OFF SOUTHERN CALIFORNIA. THE JOURNAL 21. Available at: https://swfsc.noaa.gov/publications/FED/00605.pdf [Accessed October 14, 2017].

Yoklavich, M. M., Laidig, T. E., Graiff, K., Elizabeth Clarke, M., and Whitmire, C. E. (2018). Incidence of disturbance and damage to deep-sea corals and sponges in areas of high trawl bycatch near the California and Oregon border. Deep Sea Research Part II: Topical Studies in Oceanography 150, 156–163. doi:10.1016/j.dsr2.2017.08.005.

Yoklavich, M., and O'Connell, V. (2008). "Twenty Years of Research on Demersal Communities Using the Delta Submersible in the Northeast Pacific," in Marine Habitat Mapping Technology for Alaska, eds. J. Reynolds and H. Greene (Alaska Sea Grant, University of Alaska Fairbanks), 143–156. doi:10.4027/mhmta.2008.10.

Zuur, A. F., Ieno, E. N., and Saveliev, A. A. (2017). Beginner's Guide to Spatial, Temporal and Spatial-Temporal Ecological Data Analysis with R-INLA. Volume I: Using GLM and GLMM. Newburgh, United Kingdom: Highland Statistics Ltd Available at: https://www.highstat.com/index.php/beginner-s-guide-to-regression-models-with-spatial-and-temporal-correlation [Accessed November 12, 2020].

Zuur, A. F., Ieno, E. N., Walker, N. J., Saveliev, A. A., and Smith, G. M. (2009). Mixed Effects Models and Extensions in Ecology with R. Springer.
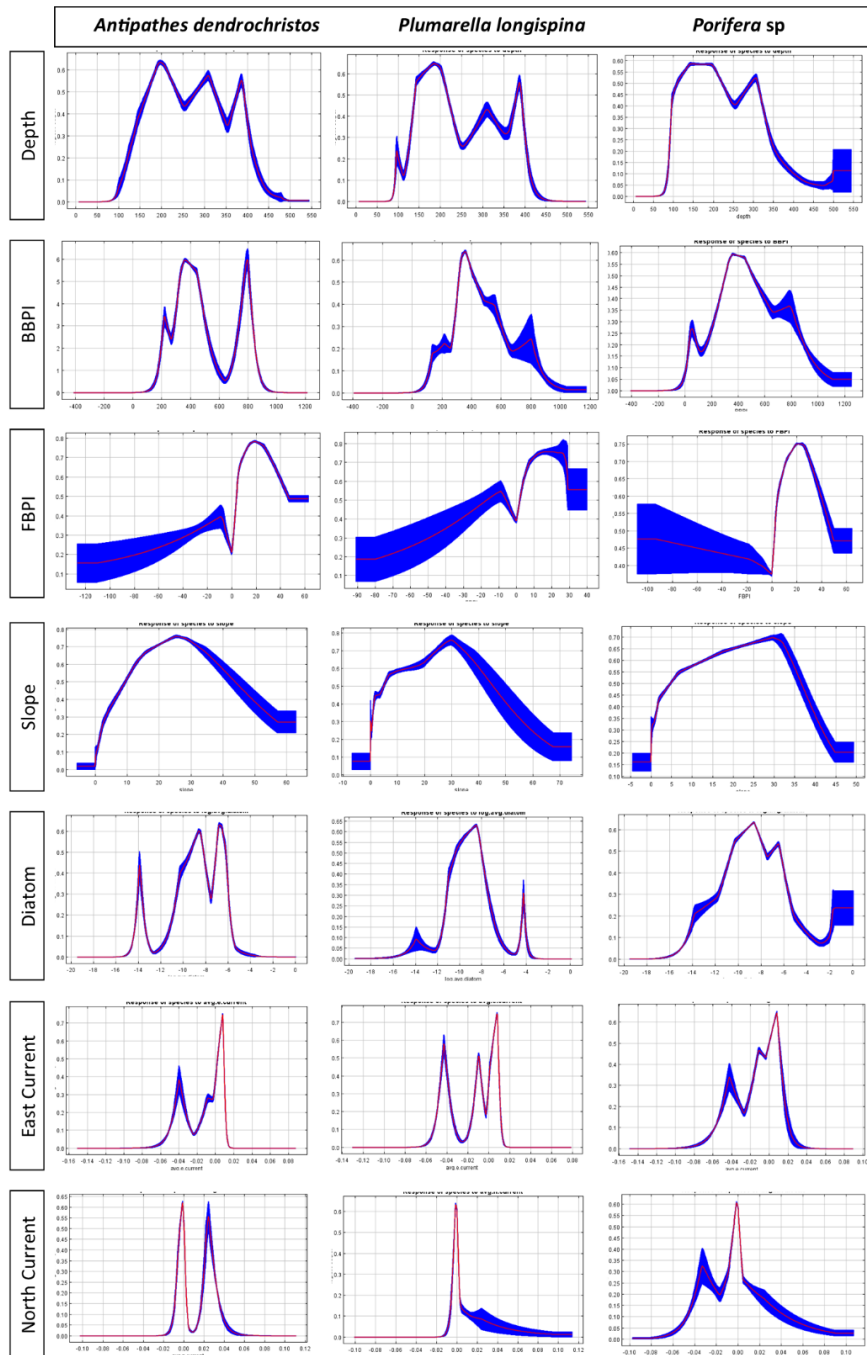
APPENDIX A

Appendix A: Supplemental Figures

Figure A1 Response plots for *Antipathes dendrochristos, Lophelia pertusa*, and Porifera sp. single variable
Maxent models. All models were made with a beta multiplier value of 0.5 and bootstrapped with
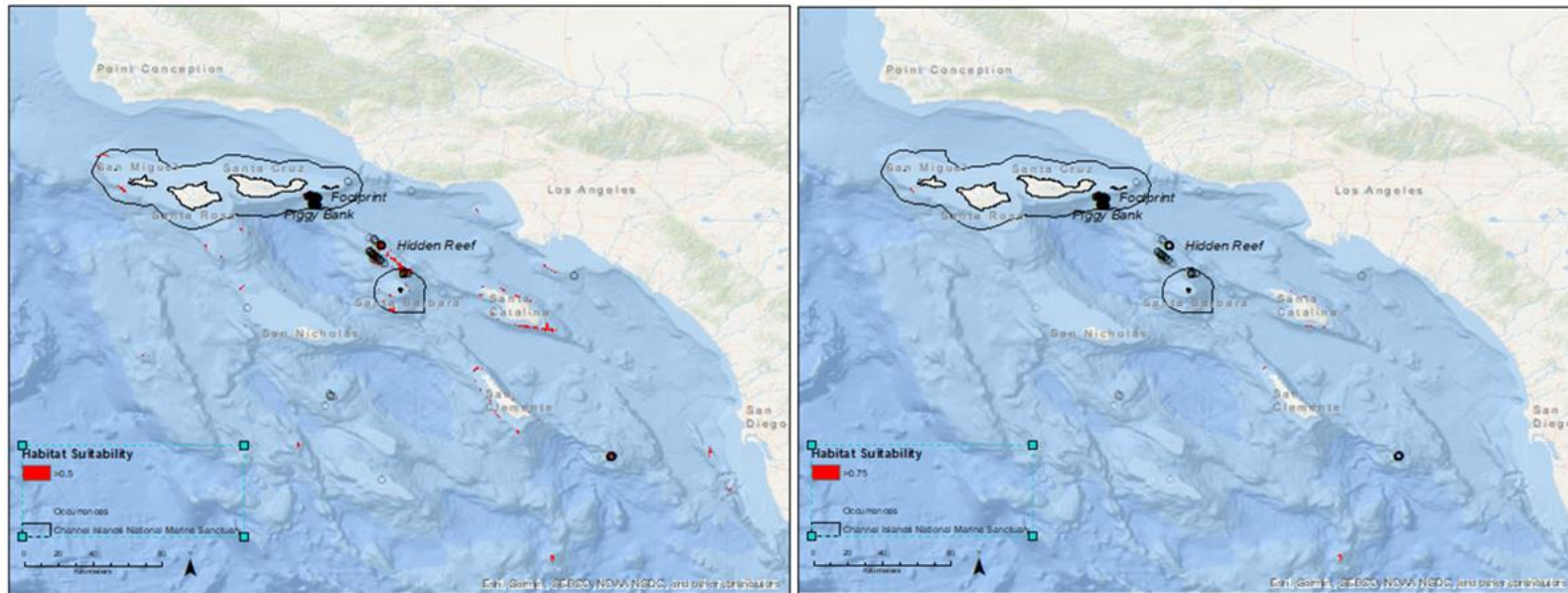100 samples.

Figure A 2 Predicted areas based on 0.5 and 0.75 logistic output thresholds for *Antipathes dendrochristos* based on maxent models.
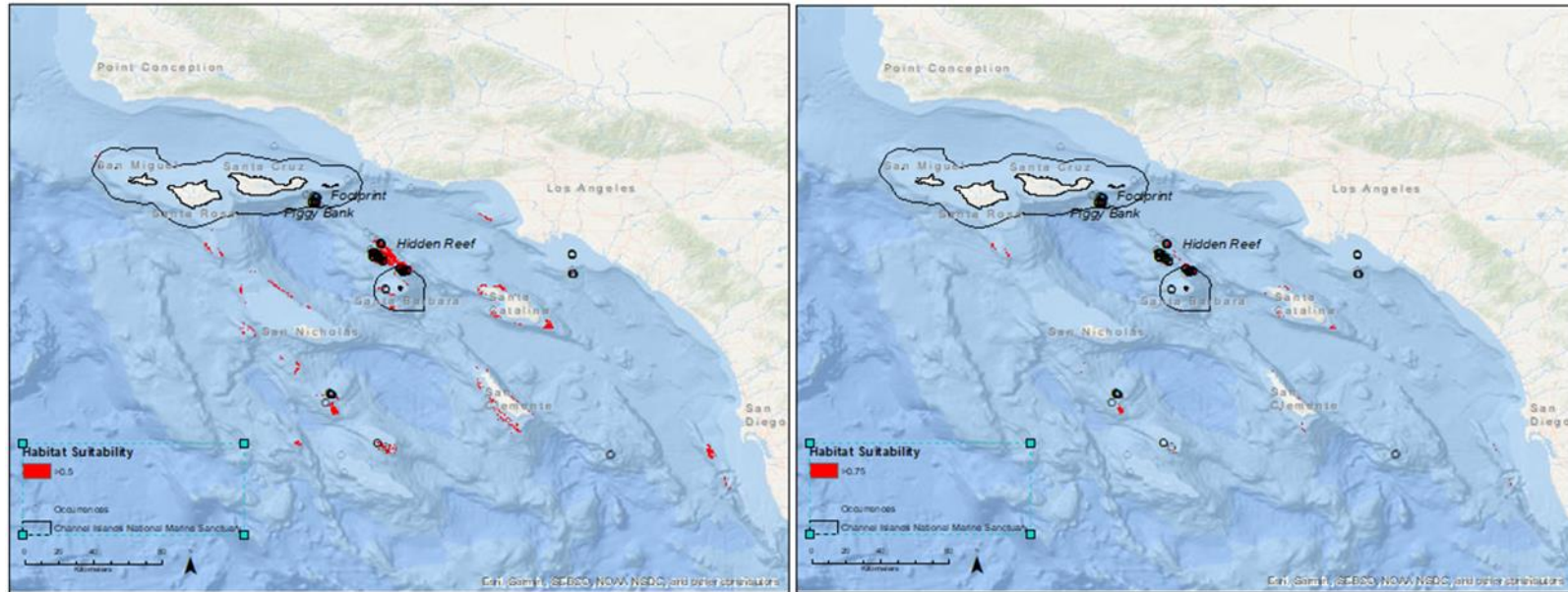
Figure A 3 Predicted areas based on 0.5 and 0.75 logistic output thresholds for *Plumarella longispina* based on maxent models.
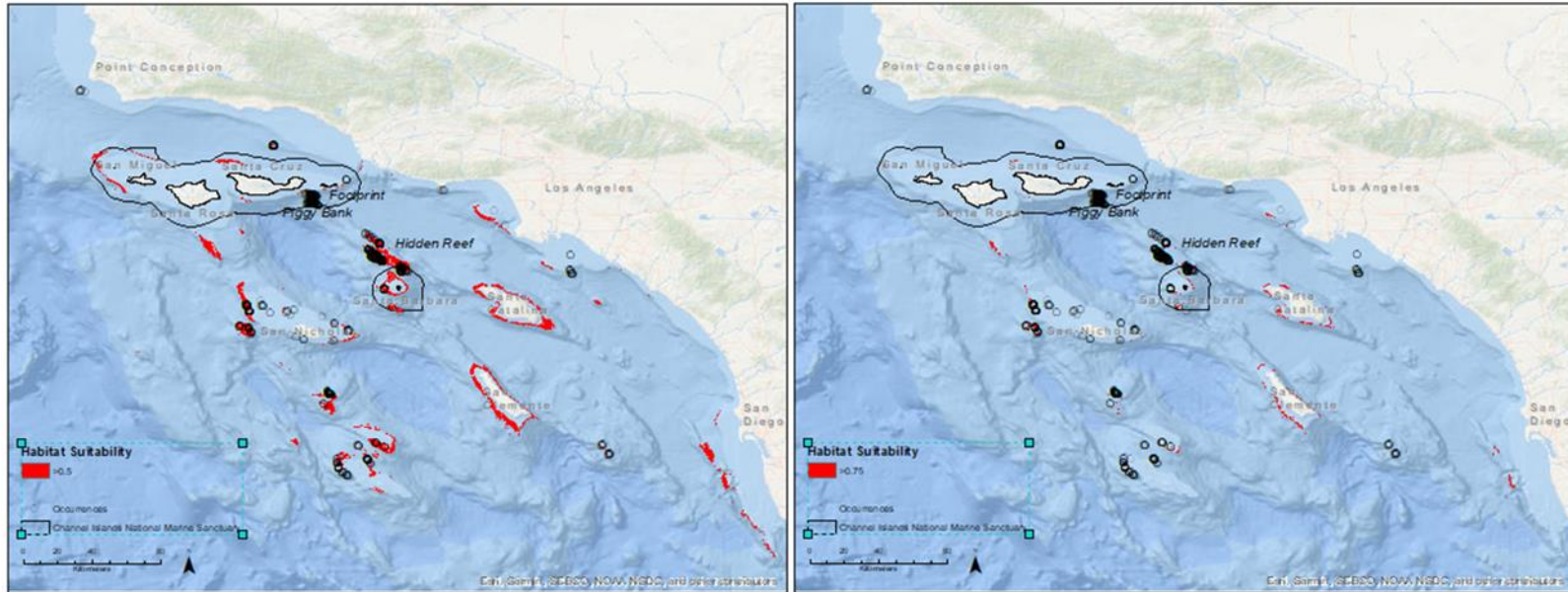
Figure A 4 Predicted areas based on 0.5 and 0.75 logistic output thresholds for Porifera sp. based on maxent models.
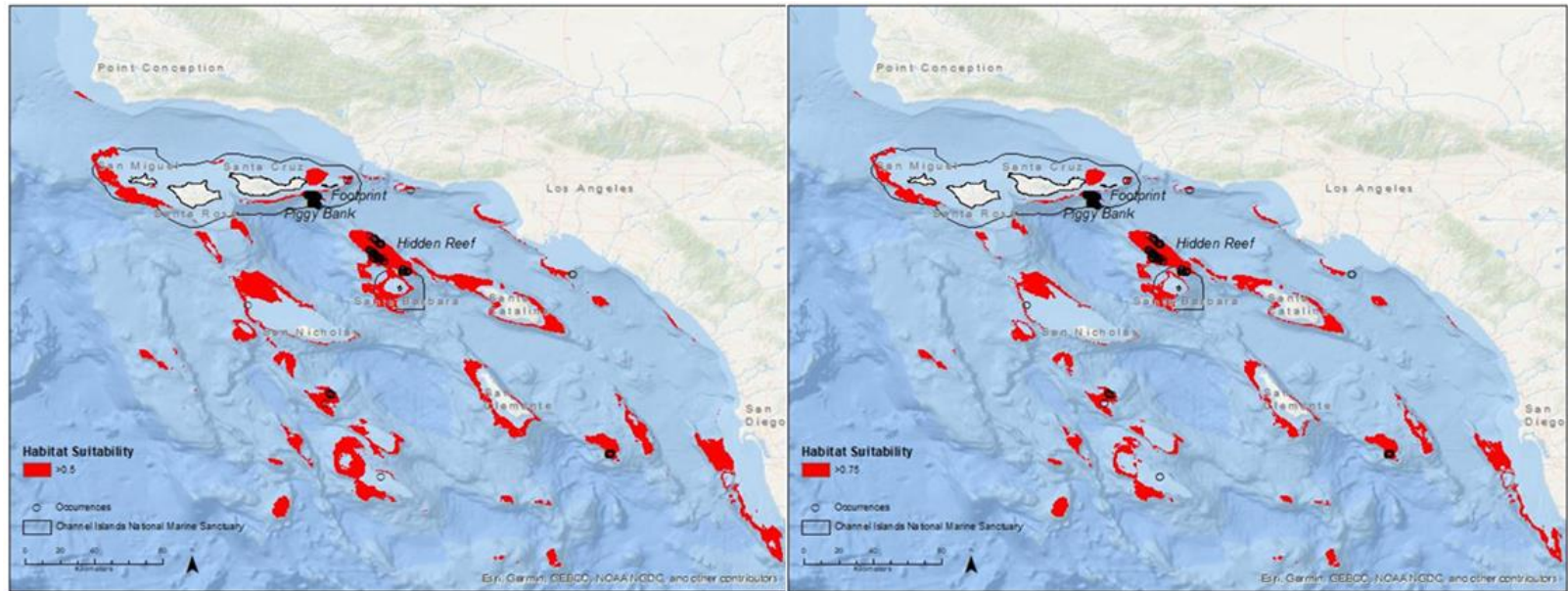
Figure A 5 Predicted areas based on 0.5 and 0.75 predicted probability thresholds for *Antipathes dendrochristos* GAMs.
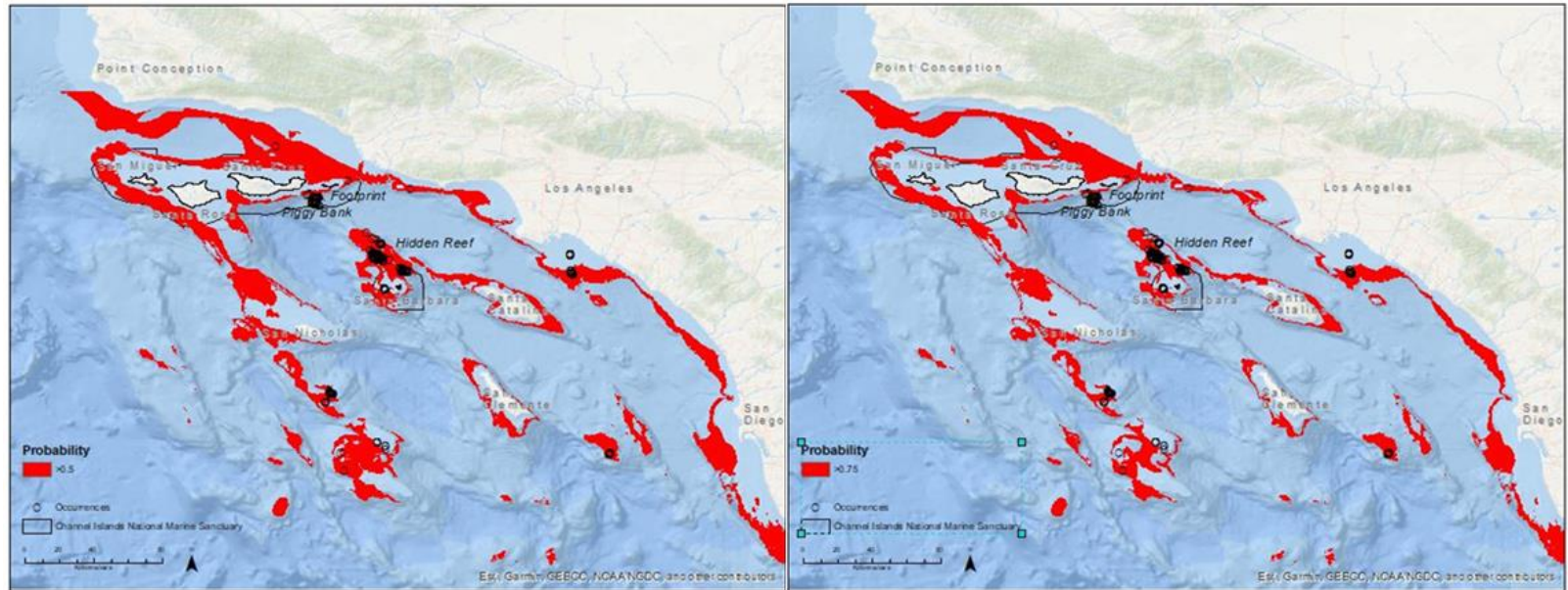
Figure A 6 Predicted areas based on 0.5 and 0.75 predicted probability thresholds for *Plumarella longispina* GAMs.
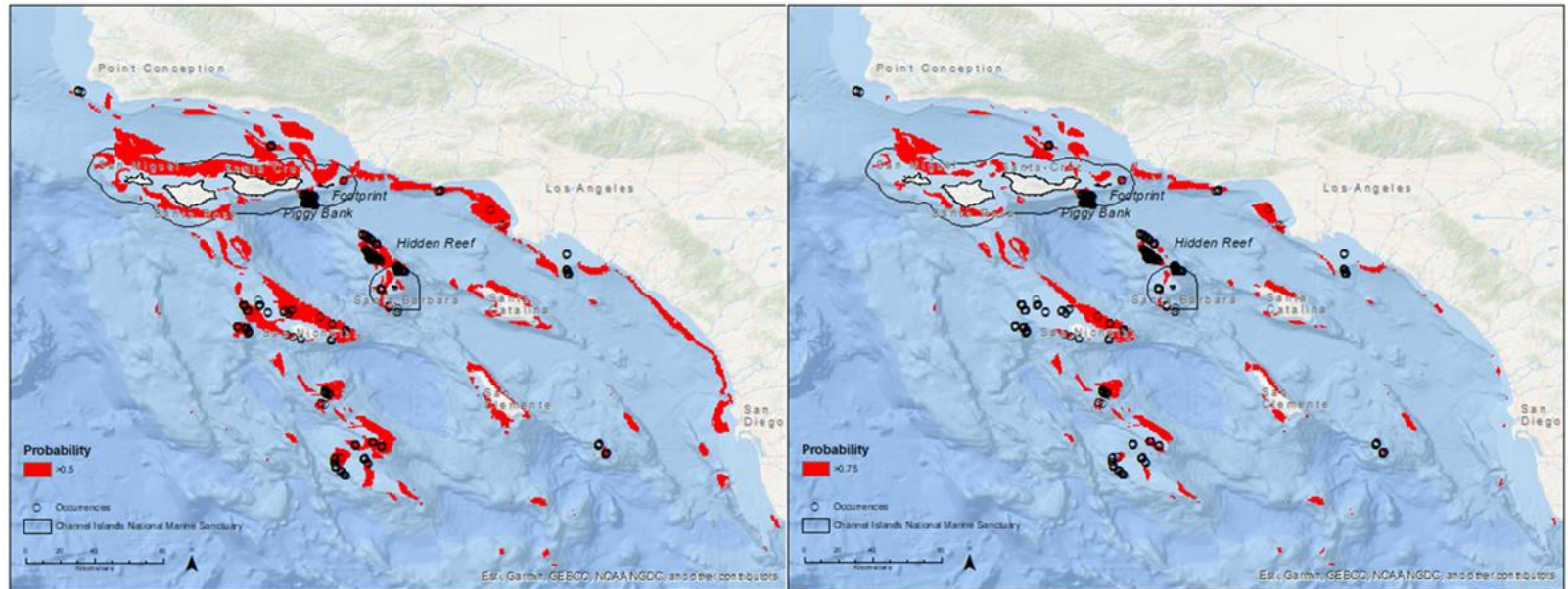
Figure A 7 Predicted areas based on 0.5 and 0.75 predicted probability thresholds for Porifera sp. GAMs.
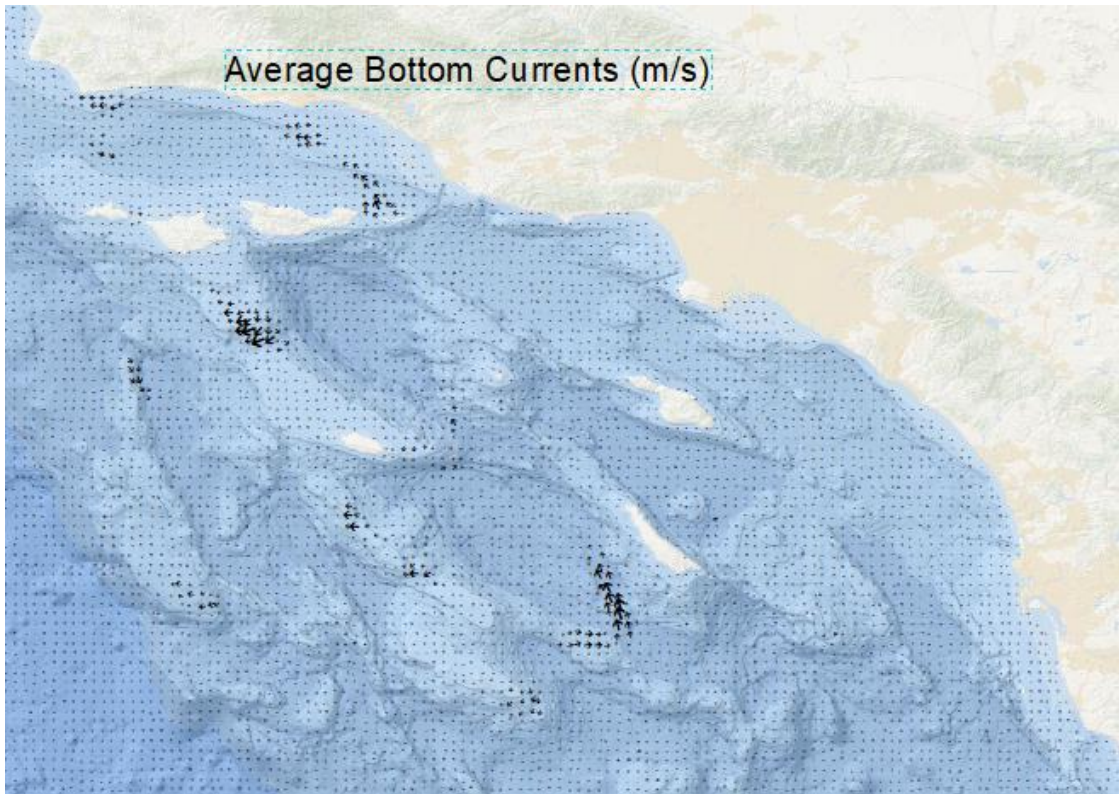
Figure A 8 Seasonal and average currents through the Southern California Bight. Areas of increased flow include the Santa Barbara Basin, on the south east end of the San Nicholas Basin, through the saddle between the banks on the west side of the Santa Cruz Basin, on the northern banks of the West and East Cortes Basins, and the bank west of the Tanner Basin.
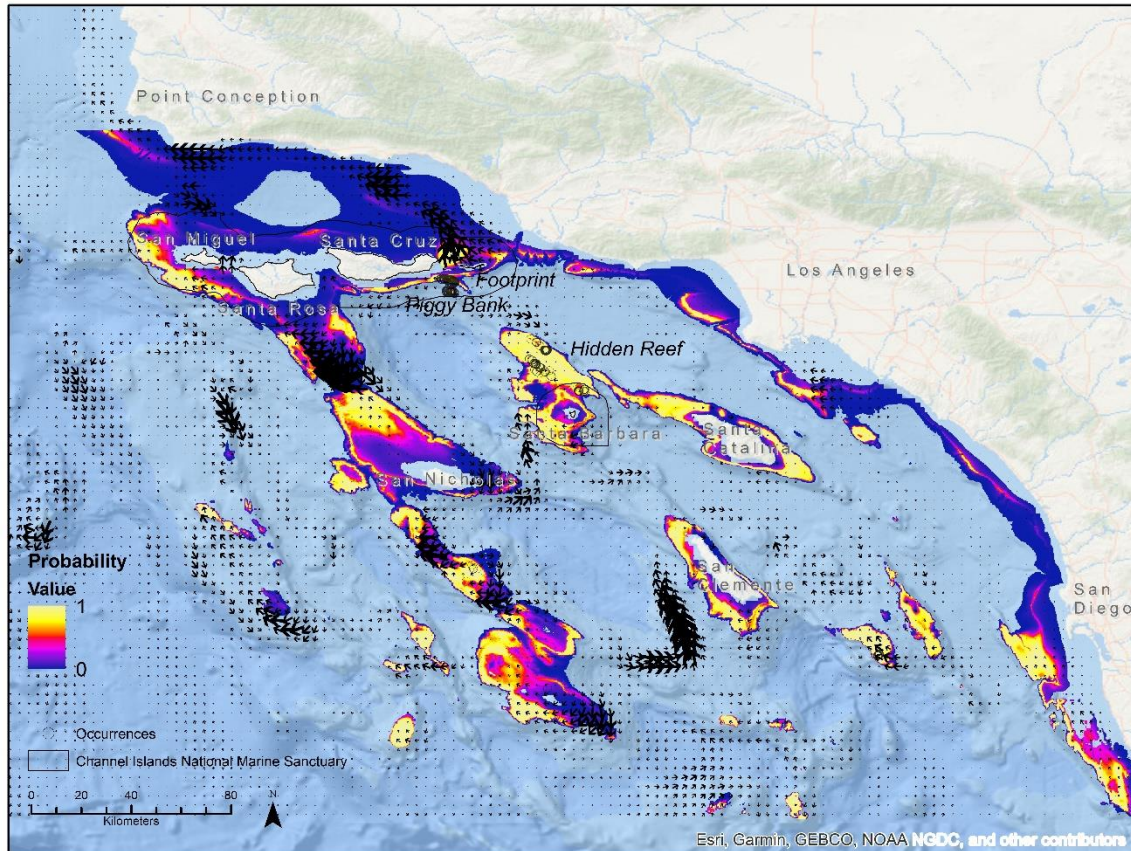
April Bottom Currents (m/s)

January Bottom Currents (m/s)

July Bottom Currents (m/s)

October Bottom Currents (m/s)
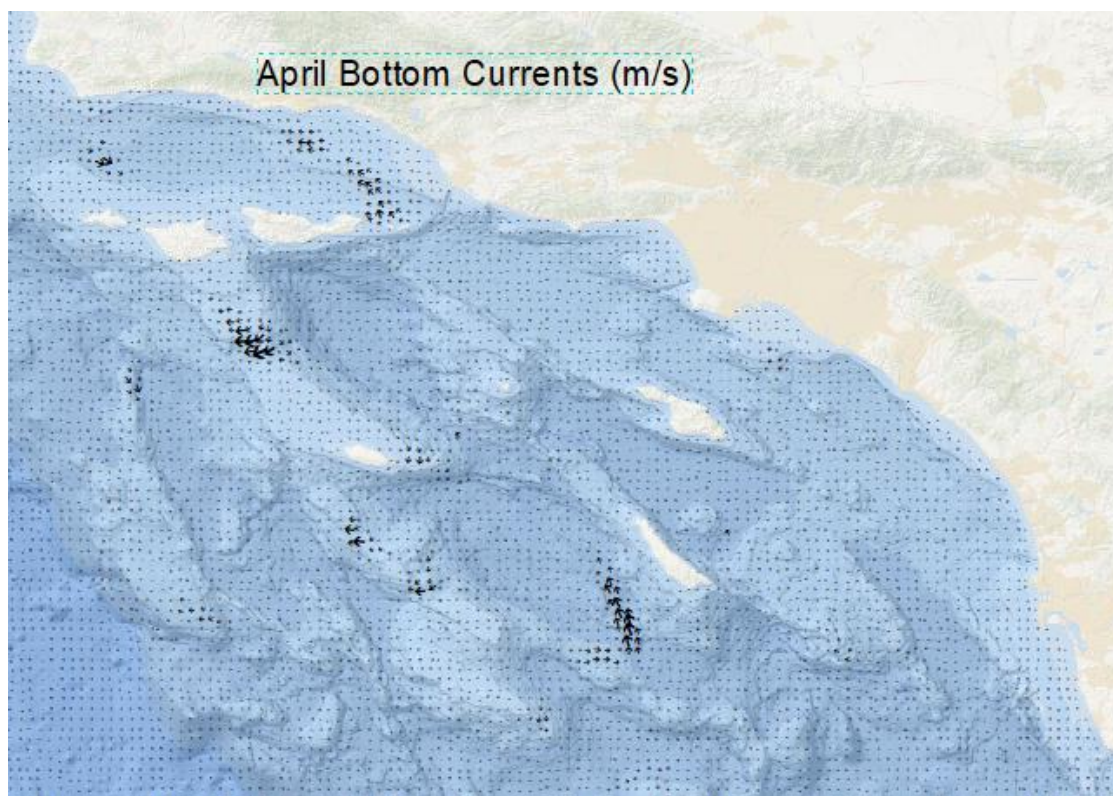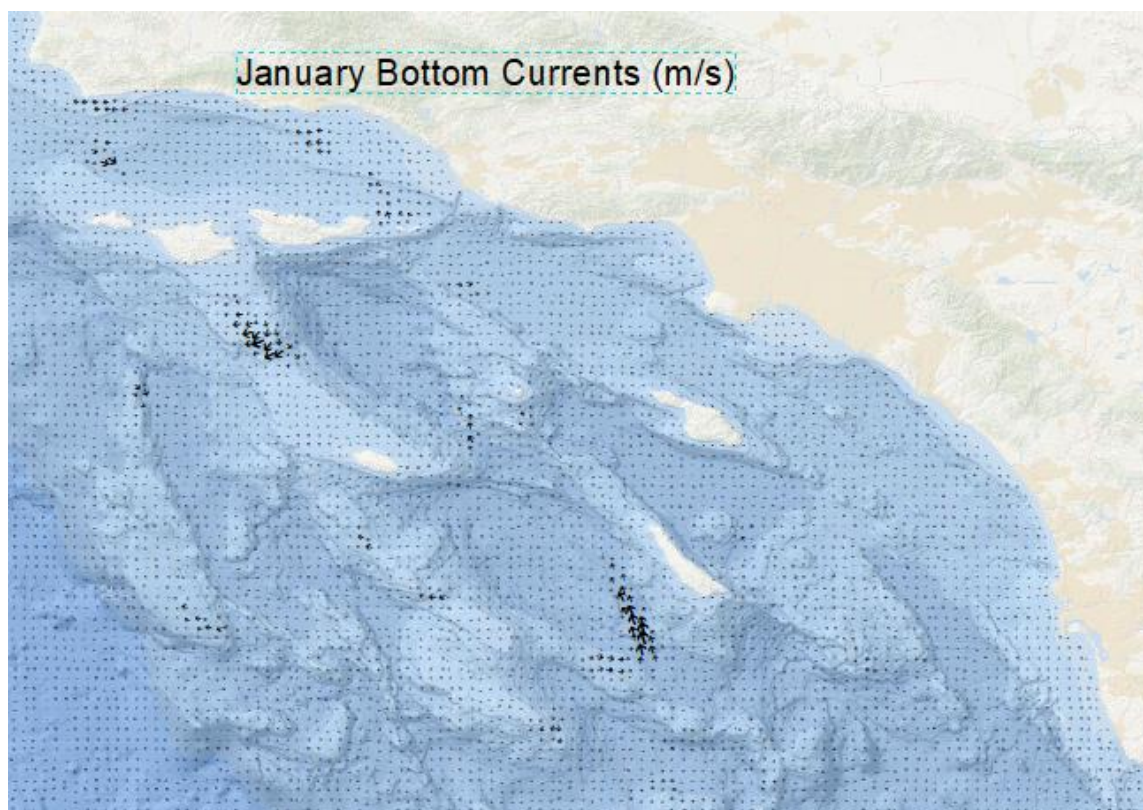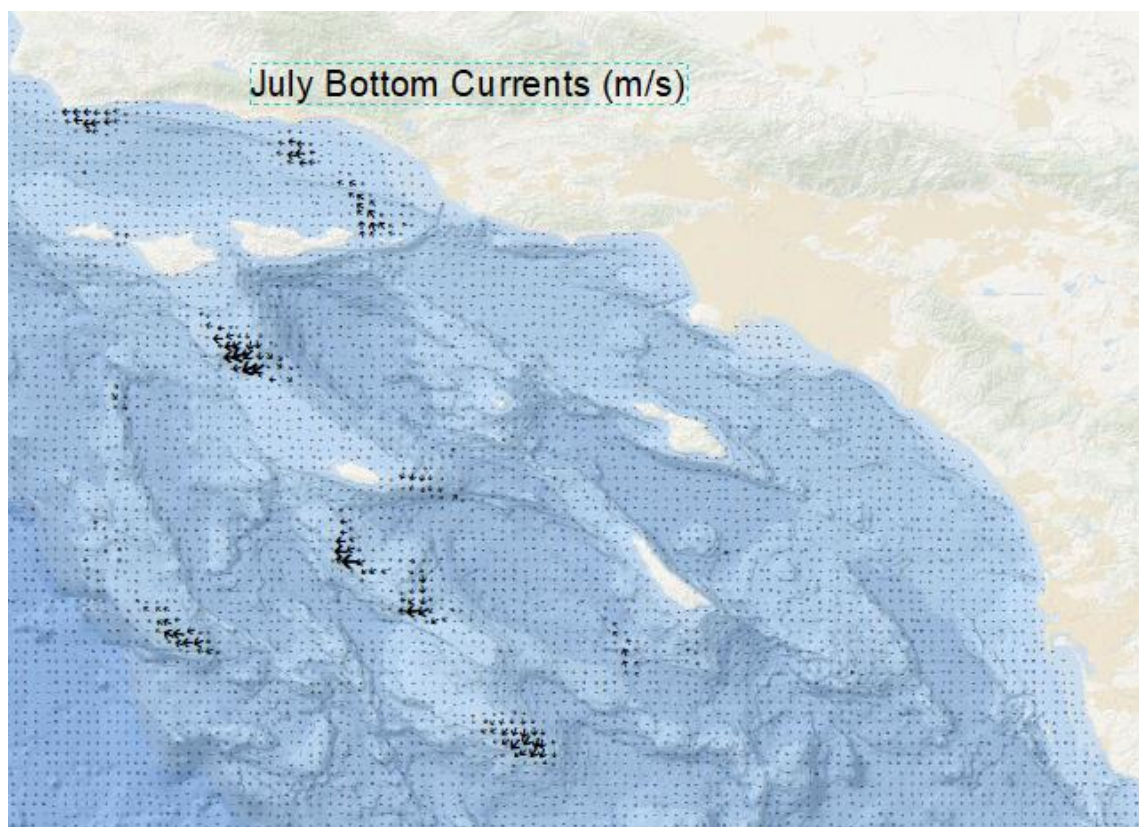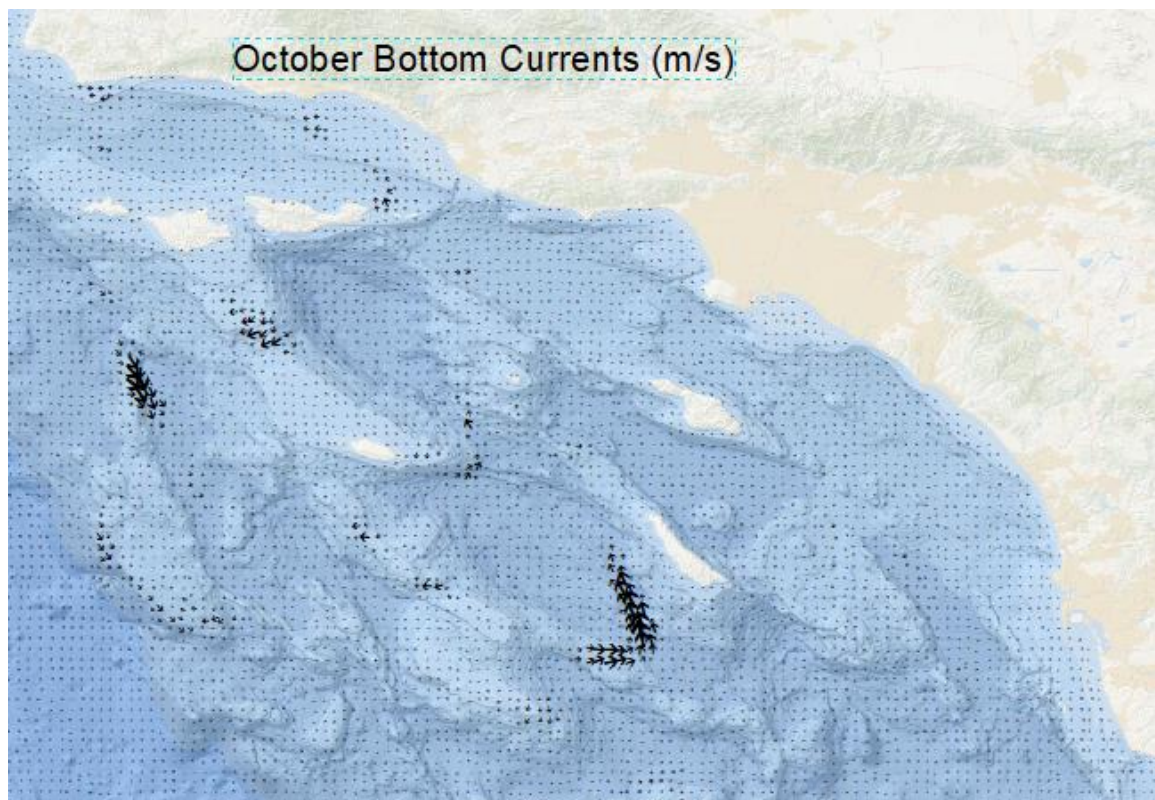
Figure A 9 GAM predictions for *A. dendrochristos* with current direction and magnitude depicted in vector form. Areas of increased flow exist east of Santa Cruz Island, through the Santa Barbara Channel, over the saddle between the banks south of Santa Rosa Island and north of San Nicholas Island, and through the banks south of San Nicholas Island.
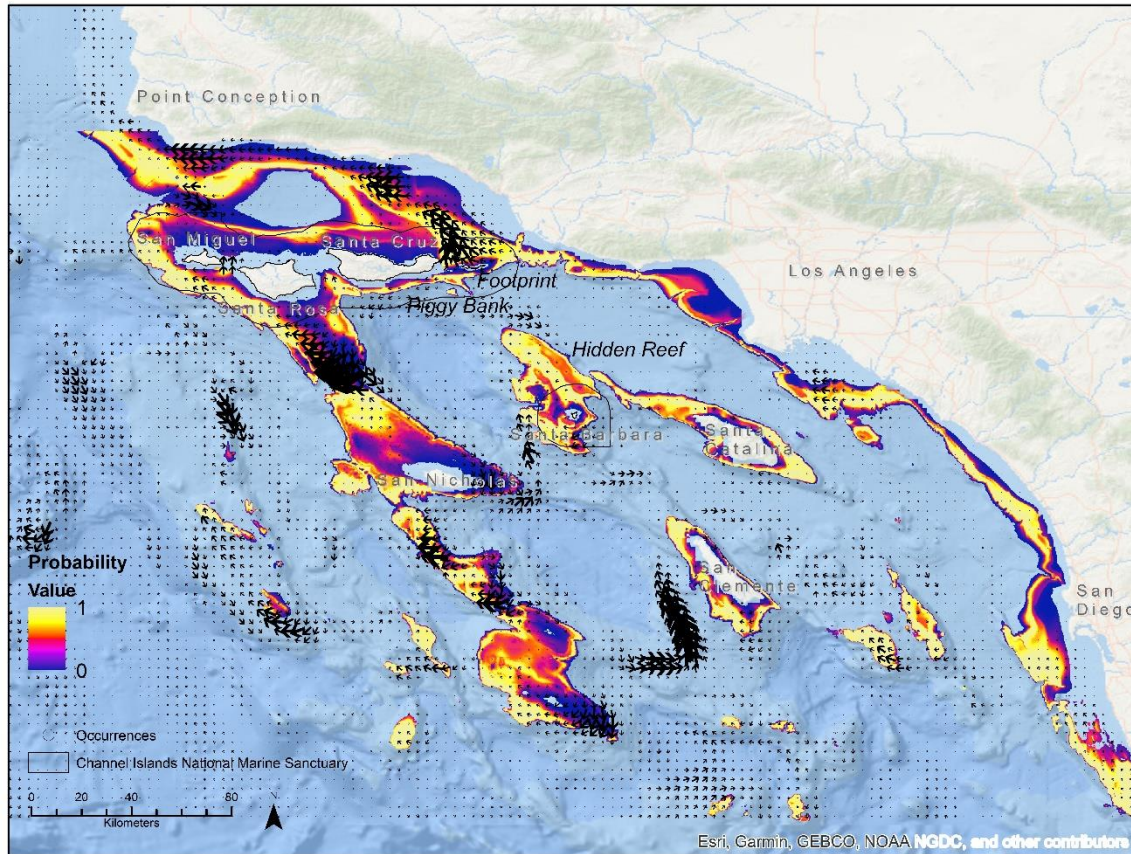
Figure A 10 GAM predictions for *P. longispina* with current direction and magnitude depicted in vector form. Areas of increased flow exist east of Santa Cruz Island, through the Santa Barbara Channel, over the saddle between the banks south of Santa Rosa Island and north of San Nicholas Island, and through the banks south of San Nicholas Island.
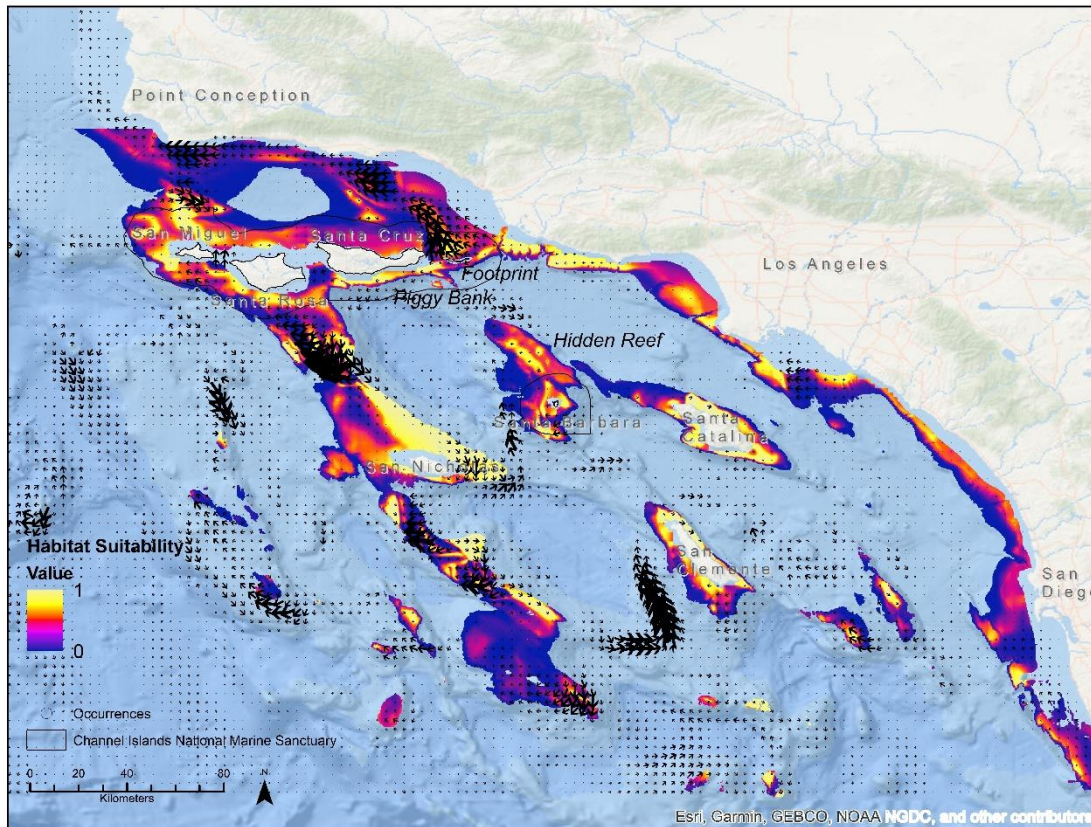
Figure A 11 GAM predictions for Porifera sp. with current direction and magnitude depicted in vector form. Areas of increased flow exist east of Santa Cruz Island, through the Santa Barbara Channel, over the saddle between the banks south of Santa Rosa Island and north of San Nicholas Island, and through the banks south of San Nicholas Island.
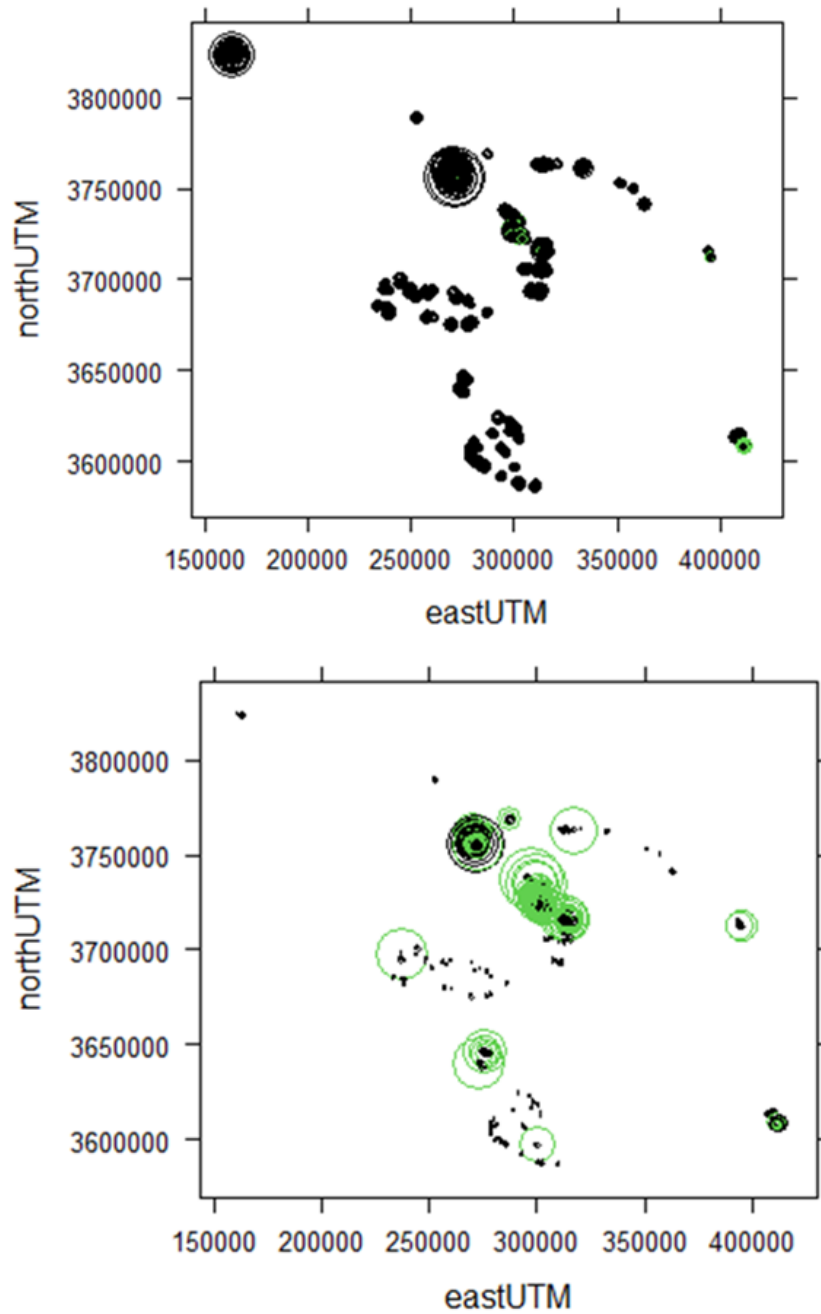
Figure A 12 Model residuals for *A. dendrochristos* for non spatial GLM (top) and spatial GAM (bottom). Black circles represent negative residuals, green represents positive. Size of circle is relative to residual magnitude.
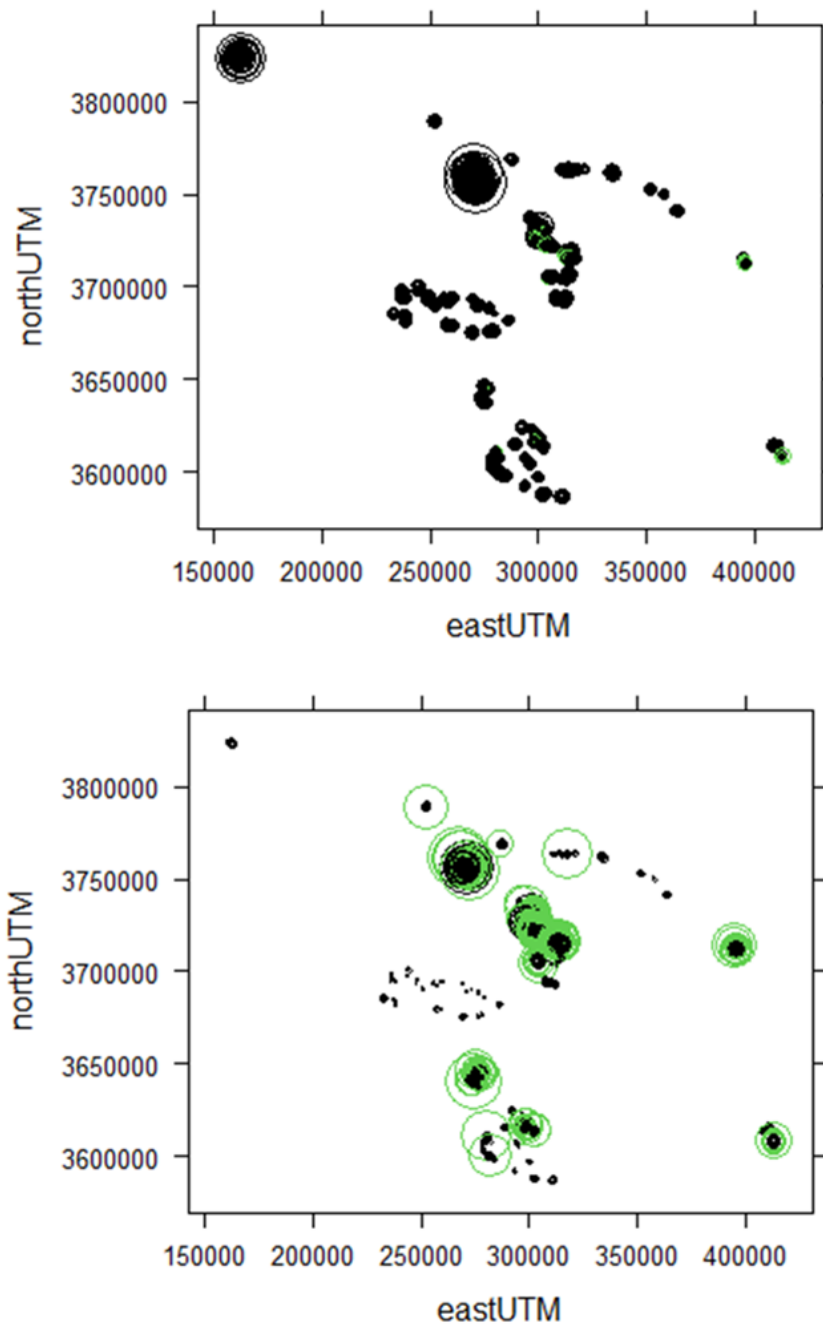
Figure A 13 Model residuals for *P. longispina* for non spatial GLM (top) and spatial GAM (bottom). Black circles represent negative residuals, green represents positive. Size of circle is relative to residual magnitude.
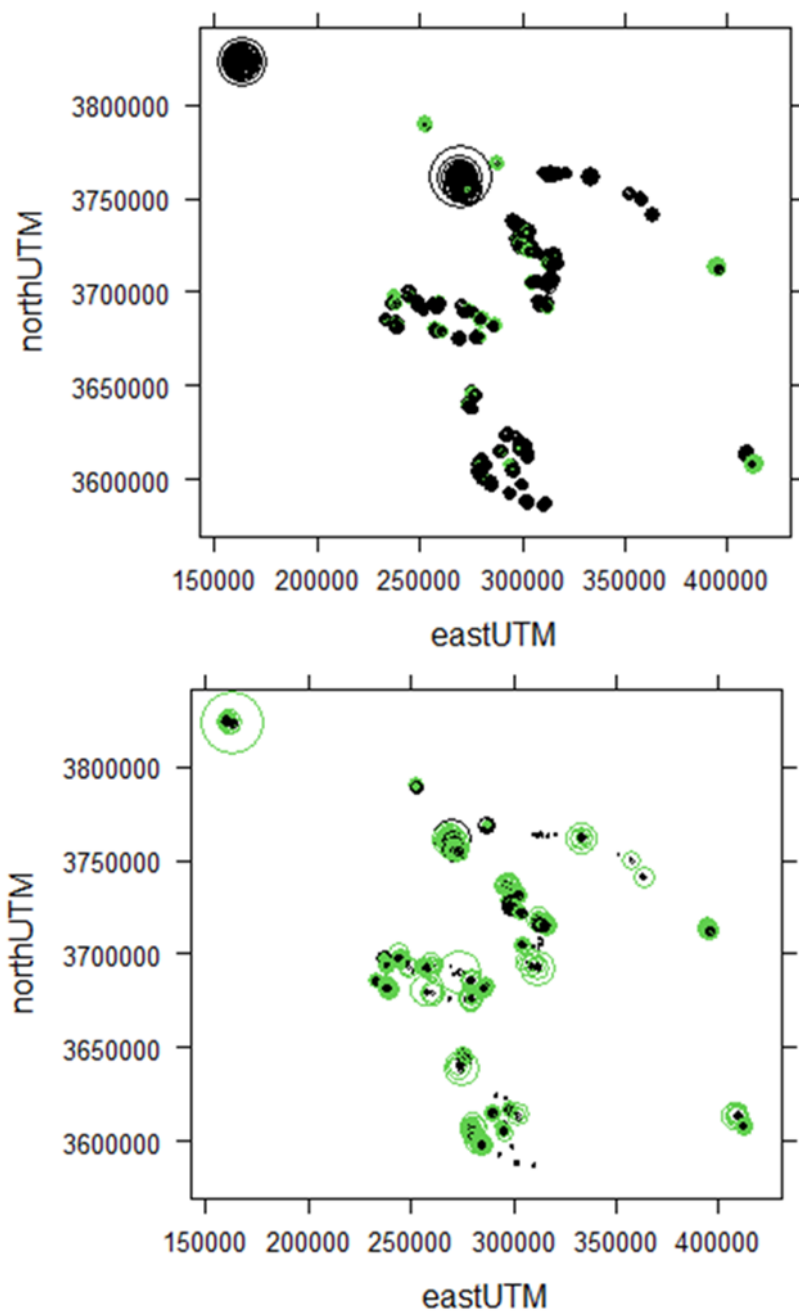
Figure A 14 Model residuals for Porifera sp. for non spatial GLM (top) and spatial GAM (bottom). Black circles represent negative residuals, green represents positive. Size of circle is relative to residual magnitude.
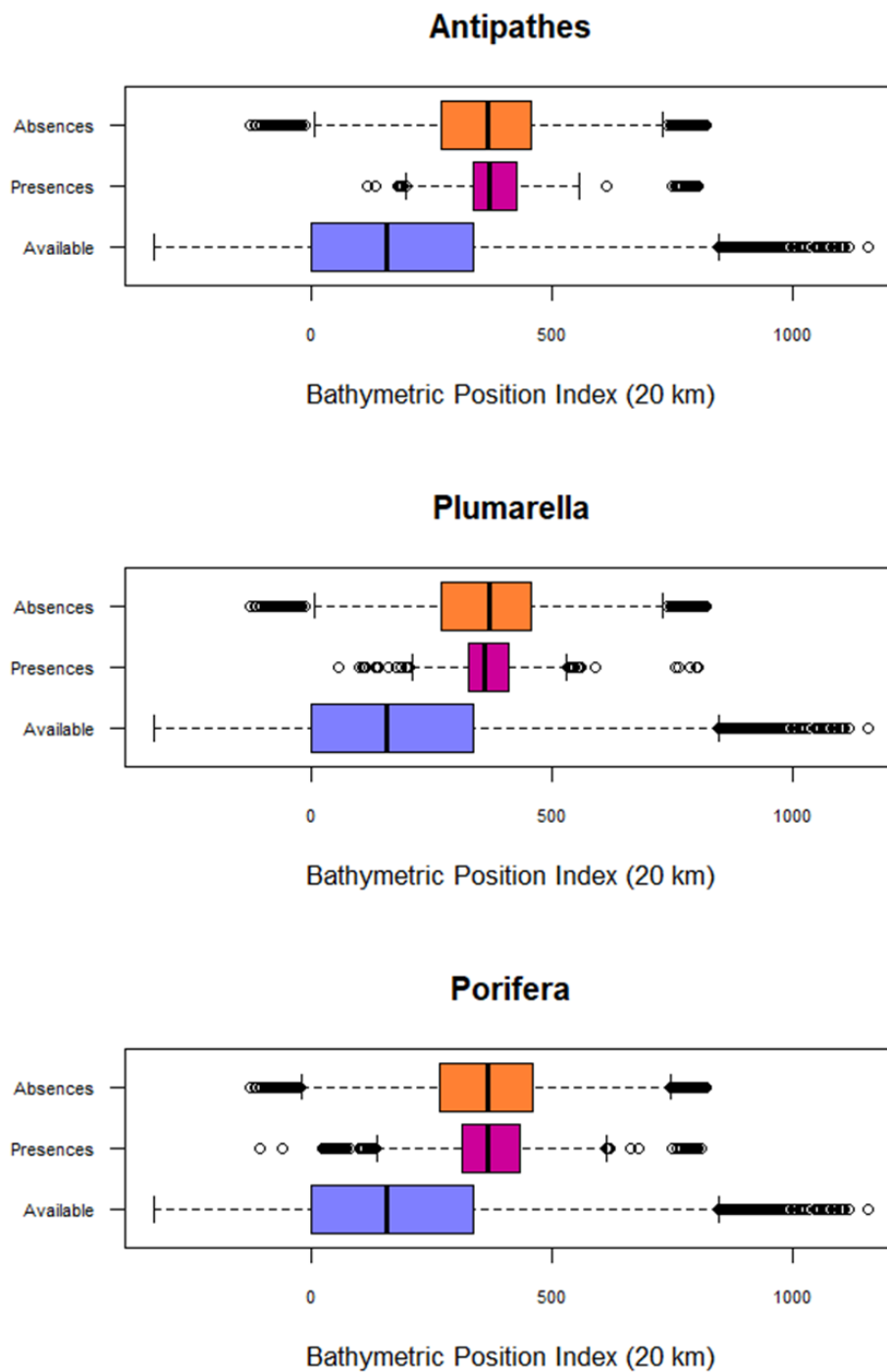
Figure A 15 Bathymetric Position Index (broad-scale) data for surveyed cells (Absence and Presence boxes) and throughout the Southern California Bight between 50 – 500 m (Available).

APPENDIX B

Appendix B: Supplemental Tables

Table A 1 Stage one of the model selection process. All combinations of smoothed and linear bathymetric variables were tested, and the model with the lowest WAIC score was used in stage two.

One Bathymetric Variable Smoothed
s(Depth) + Slope + FBPI + BBPI + Biogeophysical Variables
Depth + s(Slope) + FBPI + BBPI + Biogeophysical Variables
Depth + Slope + s(FBPI) + BBPI + Biogeophysical Variables
Depth + Slope + FBPI + s(BBPI) + Biogeophysical Variables

Two Bathymetric Variables Smoothed
s(Depth) + s(Slope) + FBPI + BBPI + Biogeophysical Variables
s(Depth) + Slope + s(FBPI) + BBPI + Biogeophysical Variables
s(Depth) + Slope + FBPI + s(BBPI) + Biogeophysical Variables
Depth + s(Slope) + s(FBPI) + BBPI + Biogeophysical Variables
Depth + s(Slope) + FBPI + s(BBPI) + Biogeophysical Variables
Depth + Slope + s(FBPI) + s(BBPI) + Biogeophysical Variables

Three Bathymetric Variables Smoothed
s(Depth) + s(Slope) + s(FBPI) + BBPI + Biogeophysical Variables
s(Depth) + s(Slope) + FBPI + s(BBPI) + Biogeophysical Variables
s(Depth) + Slope + s(FBPI) + s(BBPI) + Biogeophysical Variables
Depth + s(Slope) + s(FBPI) + s(BBPI) + Biogeophysical Variables

Four Bathymetric Variables Smoothed
s(Depth) + s(Slope) + s(FBPI) + s(BBPI) + Biogeophysical Variables

Table A 2 Stage two of the model selection process for all noncollinear variables. All combinations of smoothed and linear biogeophysical variables were tested in addition to a tensor between current variables. The model with the lowest WAIC score was used as the final model.

No Biogeophysical Variables Smoothed
Diatom Concentration + Northern Current + Eastern Current + Bathymetric Variables
Diatom Concentration + (Northern Current x Eastern Current) + Bathymetric Variables
One Biogeophysical Variable Smoothed
s(Diatom Concentration) + Northern Current + Eastern Current + Bathymetric
s(Diatom Concentration) + (Northern Current x Eastern Current) + Bathymetric
Diatom Concentration + s(Northern Current) + Eastern Current + Bathymetric
Diatom Concentration + Northern Current + s(Eastern Current) + Bathymetric
Two Biogeophysical Variables Smoothed
s(Diatom Concentration) + s(Northern Current) + Eastern Current + Bathymetric
s(Diatom Concentration) + Northern Current + s(Eastern Current) + Bathymetric
Diatom Concentration + s(Northern Current) + s(Eastern Current) + Bathymetric
Three Biogeophysical Variables Smoothed
s(Diatom Concentration) + s(Northern Current) + s(Eastern Current) + Bathymetric